

**CARRIER-ENVELOPE PHASE STABILIZED FEW-CYCLE
LASER PULSES FROM A NEON-FILLED HOLLOW-CORE
FIBER COMPRESSOR**

by

CHRISTOPHER MATTHEW NAKAMURA

B.S., The University of Michigan 2003

A THESIS

Submitted in partial fulfillment of the

requirements for the degree

MASTER OF SCIENCE

**Department of Physics
College of Arts and Sciences**

**Kansas State University
Manhattan, Kansas**

2006

Approved by:

**Major Professor
Zenghu Chang**

ABSTRACT:

Intense laser pulses are critical to studies of strong field physics, multi-photon phenomena, and attosecond pulse generation. In this work a neon-filled hollow-core fiber will be shown to, through self-phase modulation, sufficiently broaden the frequency bandwidth of a 25fs laser pulse, from a Ti:Sapphire multi-pass amplifier system, as to support pulse of ~ 6 fs duration, and that compression to such a pulse duration is attainable. It will further be shown that such a compressor can yield pulses with over 1mJ of energy. For such pulses, which contain only a few cycles of the carrier wave the carrier envelope phase offset (CEP) can present physically observable effects in physical phenomena such as above threshold ionization and high order harmonic generation. Evidence for the stabilization of the carrier-envelope phase offset using inloop and outloop f -to- $2f$ interferometry will be presented. The result, a 6.5fs laser pulse of 1.2mJ energy with rms CEP stability of 370mrad, to the best of our knowledge, represents the most CEP stable few-cycle pulses of this energy and short duration to date. Progress towards the measurement of the absolute carrier-envelope phase using the technique of high harmonic generation is presented. These results open up new possibilities in ultrafast laser science.

“To know that we know what we know, and to know that what we don’t know we don’t know, that is true knowledge.”

-Nicholaus Copernicus

Table of Contents

List of Figures	iv
Acknowledgements	vi
Preface	ix
Chapter 1: Introduction	1
Chapter 2: Theory of Self Phase Modulation	8
2.1 The Nonlinear Propagation Equation	8
2.2 The Broadening Factor	11
Chapter 3: The Carrier-Envelope Phase Offset	13
3.1 The Theory of the Carrier-Envelope Phase	13
3.2 CEP Locking Apparatus of the KLS Oscillator	18
3.3 Feedback Correction of the CEP Drift in the KLS Amplifier	20
Chapter 4: The Hollow-Core Fiber Compressor Experiment	24
4.1 The Experimental Apparatus	24
4.1.1 The Kansas Light Source Laser System	24
4.1.2 The Hollow-Core Fiber Compressor	25
4.1.3 Stabilization of the KLS Laser Power	26
4.2 Beam Characterization	27
4.2.1 Coupling Efficiency and Mode Quality	27
4.2.2 Spectral Broadening	30
4.2.3 Pulse Duration	33
4.2.4 The Carrier-Envelope Phase Drift	36
Chapter 5: FROG as a Diagnostic Tool for Ultrafast Lasers	40

5.1 The Autocorrelator	40
5.2 Frequency Resolved Optical Gating (FROG)	43
5.2.1 General Principles of FROG	43
5.2.2 Practical Alignment and Calibration of FROG	47
Chapter 6: Application of Neon Fiber to HHG CEP Measurement	50
6.1 Modeling HHG	50
6.2 HHG Experimental Apparatus	53
6.3 Preliminary CEP Data	59
Chapter 7: Conclusions and Future Work	61
7.1 Conclusions	61
7.2 Future Work	61
7.2.1 Pressure Gradient Fiber	62
7.2.2 Pulse Compression via Filamentation	63
7.2.3 Further HHG Investigations	64
References	66
Associated Publications	69

List of Figures

Fig 1.1 Effect of CEP on electric field amplitude for two pulses	4
Fig 3.1.1 Effect of CEP on electric field amplitude for two pulses	13
Fig 3.1.2 Frequency Comb of a Laser Oscillator	15
Fig 3.1.3 Coherent Superposition of Eigenmodes	17
Fig 3.2.1 Schematic of KLS Oscillator CEP Locking Mechanism	20
Fig 3.3.1 Colinear f -to- $2f$ Interferometer	22
Fig 4.1.2.1 The Kansas Light Source Laser System	24
Fig 4.1.2.2 Hollow-core fiber apparatus	26
Fig 4.2.1.1 Output Energy vs. Input Energy	27
Fig 4.2.2.1 Beam Profile and Mode Quality	30
Fig 4.2.2.2 The Full Width of an SPM Broadened Spectrum	31
Fig 4.2.2.3 Spectral Broadening vs. Pressure	32
Fig 4.2.2.4 Amplifier Spectrum and Optimized Output Spectrum	33
Fig 4.2.3.1 FROG Trace and Reconstructed Pulse Duration	35
Fig 4.2.4.1 Stereoscopic ATI Phasemeter Data	36
Fig 4.2.4.2 f -to- $2f$ Fringes for Ne Fiber CEP	38
Fig 4.2.4.3 In-loop and Out-loop CEP for Ne Fiber	40
Fig 5.1.1 Schematic of an Autocorrelator	42
Fig 5.2.1.1 Schematic of a FROG Apparatus	44
Fig 5.2.1.2 FROG Single-Shot Delay Geometry	46
Fig 5.2.2.1 Calibration of the Spectrometer	48
Fig 5.2.2.2 Determining the Delay Step Size	49

Fig 6.1.1 HHG 3-Step Process	51
Fig 6.2.1 The XUV Spectrometer	54
Fig 6.2.2 HHG Electronics Flow Chart	56
Fig 6.2.3 HHG Electronics Synchronization	57
Fig 6.3.1 Preliminary HHG CEP Data	60
Fig 7.1.1 A Hollow-Core Fiber Compressor with a Pressure Gradient	63
Fig 7.2.1 A Filamentation Compressor Apparatus	64

ACKNOWLEDGEMENTS

The completion of a degree, or a project can be a very satisfying event. When we come to the close of something for which we have worked hard, and struggled it gives us a moment to pause and take stock of what we have done, and what we have become. In that spirit it is also necessary to pause, and give thanks to those who have helped us do those things, and are very much a part of who we are.

I am first and foremost indebted to my advisor Zenghu Chang whose seemingly inexhaustible patience, expertise, and spirit of experience-based learning have helped me to pursue research much more aggressively and assertively than I could have imagined. He has served as a model example of the modern laser scientist, and has enabled me to understand the research process in a far deeper way than I did before. Zenghu, I thank you for giving me the opportunity to take part in this research.

Of course it takes a village to raise a child and it takes a faculty to graduate a student. I would like to acknowledge Brian Washburn and thank him for his advice, assistance, and time, which he offered so generously. Discussions with Brian have helped me in this work profoundly, but perhaps more importantly has helped to see beyond the lab, and look at how one finds ways for science and “real life” to coexist. I would like to thank Larry Weaver discussions related to...too many things to mention. I also thank Kristan Corwin, Lew Cocke and Amit Chakrabarti for their insights in and beyond the lab.

The Kansas Light Source is a unique place to work, where a single experiment frequently involves controlling more parameters and, feedback loops, or operating more

equipment than one person could ever do by themselves, and as such I feel there is a rich atmosphere of collaboration amongst the students and post-doctoral researchers who work there. I wish to express my high regard for, and gratitude to those who worked with me in the trenches, on this work, and other projects. I feel compelled to begin with Hiroki Mashiko who has taught me more about laser science than I have room to describe, I feel honored and privileged to have worked with him. ありがとうございます増子様! Cheng Quan Li must be recognized for generously sharing his understanding of many things with me, most importantly CEP stabilization, and for making our work together so pleasant. He must also be thanked for unlocking secret menu items at Happy Valley. Steve Gilbertson, Mahendra Shakya, Eric Moon and Wang He, have been extremely enjoyable to work with, and I feel much richer for the experience. In particular the chalkboard talks with Steve and Mahendra will not be forgotten.

I must also acknowledge students outside the KLS who have helped me to keep my sanity when sleep was scarce and discuss my research problems when I was looking at them too closely for my own good. Of these there are many, but three stand out in my mind always. Marc Trachy, Dipanwita Ray, and Max Sayler, thank you so much for all your help, advice and friendship.

This is getting long, and I know they will never read this, but I feel heavily indebted to those for whom I've worked for in the past. Again a few really stand out: Jason Engbrecht, Mark Skalsey, Elizabeth Batteh, and Ralph Conti. I valued the experience of working with them a great deal at the time, and later came to realize I had actually undervalued it. Along a similar vein I should take a minute to acknowledge Jens

Zorn and his cousin George who tried to teach me how to make the best of what was available for me, and who demanded that I put the cookies on the table when I wanted to put them on the highest shelf. I reflect on his teachings regularly, and they always remind me I have a very long way to go, and that that's okay.

Lastly there was life before grad school (as there will be again!). I would be nowhere without the generous emotional support of my family, in particular Sarah Nuss-Warren, my parents Alice and Scott, and my brother Joshua.

Preface

The wave-particle duality, as it must be applied to light is a testament both to the precision that humankind's scientific investigations can achieve, and the earnest, and steadfast spirit in which these scientific investigations have historically been undertaken. The fact that the electromagnetic field is quantized, and the interaction between two charged particles is mediated by the exchange of a particle of light, a photon, and the fact that we know this, is truly amazing. And we do know this. Quantum Electrodynamics is perhaps the best tested theory in modern physics. Certainly this quantization is a difficult abstraction to make. It is also an abstraction rich with conceptual implications. It is most likely for these reasons that it was deemed worthy of at least two Nobel Prizes, but this is unequivocally not the reason why it is amazing, in the author's opinion. The reason is simply that classical field theory and wave mechanics does such a superb job of describing so much of light's behavior, and that so much progress towards understanding and even controlling light can be made without ever invoking such a thing as a "photon".

Certainly when laser scientist point their lasers at atomic or molecular systems they frequently envision the absorption or emission of one, two, or many photons by an atom or molecule, and certainly when they think about their detectors, many of which work by the photoelectric effect, they speak of photon flux, but when designing cavities, building laser systems, generating, tailoring and measuring laser output both CW and pulsed, no one thinks or speaks of photons. Such efforts are work on the border between two fields, the classical and quantum. Quantum mechanics hints at its existence in the population inversion we introduce in the atoms, but after that it's a story about electromagnetic boundary conditions and Maxwell's wave equation. It's a case of

classical waves in a classical cavity propagating by way of classical fields. Furthermore it's a pretty convincing story, even by the standards of physical science.

This work is a small part of that story. It is the story of the generation and measurement of laser pulses only a few optical cycles in duration. Pulses generated for the purpose of probing the quantum world by superposition of waves created in the classical world. These light pulses are so short, and their interaction with the material world so strong (and to a significant extent classical) that changes in the electric field itself, as opposed to simply the intensity profile, can produce measurable changes in the results of an experiment. As a result the electric field of these laser pulses must be at least reproducible from laser pulse to laser pulse, and preferably controllable. This is then by necessity a story of measuring the properties of these pulses, and feeding back our measurements to exercise control all the way down to the phase of laser field.

The control of light is nothing new; you can do that with a lens and a candle or the sun. This was a technique for ignition well known to the ancient Greeks. Controlling alternating electric fields is also not new; this was done over a hundred years ago. What is new is combining the two: controlling light by controlling the field itself and doing so in pulses of light, which contain only a few oscillations. This is a step towards exercising control in the quantum world of electrons, atoms, and molecules. The precision with which we control our laser pulses is then a measure of the precision with which we can exercise control of quantum wavepackets. As science and engineering naturally spur each other on, each encouraging the efforts of the other, the natural conclusion of this statement is clear: if you can control the quantum wavepackets of electrons you can control chemistry –atom by atom, molecule by molecule. You can build structures –a

few atoms in size. It is no overstatement that this classical control of electric fields is the gateway to control of quantum interactions.

It is both amazing and useful that we know that the electromagnetic field is a quantum phenomenon. It is arguably, equally amazing, just how far you can get in the description and control of light without even asserting that knowledge.

Chapter 1: Introduction

The physical processes of nonlinear optics, and in a sense much of atomic physics in general, can be roughly classified based on the laser intensities at which the processes occur and saturate[1]. It is therefore important to the study of nonlinear optics and atomic physics to have control over the intensity of the laser used to excite the system. Since modern studies in these fields of interest are frequently conducted with pulsed lasers we should consider the intensity of a laser pulse. The peak intensity of a pulsed laser at its focus is given by

$$I_{peak} = \frac{2E}{\tau_p \pi w_0^2} \quad (1.1)$$

where E is the pulse energy, τ_p is the pulse duration, and w_0 is beam waist. Thus for a fixed focus spot size set by the diffraction limit, we see that control of the laser intensity translates to control of the pulse energy and temporal duration. Chirped Pulse Amplification (CPA) has made the generation of laser pulses with mJ energy and tens of femtosecond (fs) duration possible[2]. It is, however desirable for several reasons to have pulses of shorter duration. The first reason is that shorter laser pulses provide a faster interaction time when directed into matter, and thus can be used to study phenomena, which occur on faster time scales. The second reason is that shorter pulses of the same given energy are more intense; thus, shorter pulses can open up previously inaccessible physical phenomena in ultrafast and nonlinear optics.

The most established method of generating few cycle pulses from amplified Ti:Sapphire laser systems at this time is the hollow-core fiber compressor, first produced in 1996 by Nisoli et al[3]. In such a compressor a long pulse ($\tau_p \sim 10\text{fs}-100\text{fs}$) is passed

through a small hollow glass waveguide (hollow-core fiber) containing a rare gas. The waveguide maintains high laser intensity across the interaction length. As the laser pulse passes through the gas its intensity in the medium affects the index of refraction of the medium, which in turn impacts the phase of the pulse itself. Since a frequency is nothing more than the derivative of a phase this process, Self-Phase Modulation (SPM), can introduce new frequencies into the pulse spectrum. Under the proper conditions this results in a broadening of the laser pulse's spectral bandwidth. Reflecting these spectrally broadened pulses off a matched chirp mirror set introduces negative dispersion, This compensates for the positive dispersion, and its temporal broadening effect, that the pulse accrues by passing through the rare gas, air, glass, and any other dispersive media in the set-up. Such compressors coupled with Ti:Sapphire amplifiers have resulted in pulses as short as 5fs with a carrier wavelength of around 800nm and pulse energies up to 1mJ[3-6]. Ionization of the gas, and plasma defocusing ultimately place limits on how much pulse energy can productively be directed through the hollow-core fiber compressor. Therefore, although early efforts [3-5] mainly focused on Ar gas as a nonlinear medium, Ne gas, as used in [6] and this work presents an advantage in the form of a higher ionization potential. The ionization potential of Ne is 21.559 eV. Ar has an ionization potential of 15.755eV. It is this large difference in ionization potential that allows significantly more pulse energy to be applied to a Ne fiber. In the case of the KLS facility an Ar fiber is pumped with at most 1.3mJ of energy, while the Ne fiber was pumped to as much as 2mJ without saturating the spectral broadening effect.

For the laser intensities considered in this work ($\leq 10^{15}$ W/cm²) a laser pulse can effectively be viewed as an electric field, which contributes to the interaction, and a

magnetic field, which does not. The effect of the magnetic field must also be considered at higher intensities, but will not be in this work. In this case we can mathematically express the electric field of a laser pulse as the product of a complex envelope function, $A(z,t)$ which determines the pulse profile and a complex carrier wave, which determines the fast scale oscillation of the electric field:

$$\tilde{E}(z,t) = A(z,t)\exp(-i(k_0z - \omega_0t + \phi)) \quad (1.2)$$

For laser pulses containing many cycles of the carrier wave the physics of the laser-matter interaction can largely be determined by knowledge of its temporal duration and its intensity profile, that is knowledge of the envelope function. These properties alone will dominate in predicting the physical interaction of the pulse with a material system. Things are not so simple for pulses, which contain only a few cycles of the carrier frequency. For such pulses the electric field itself can play a role in determining the dynamics of the physical interaction. As such, a phase shift of the carrier wave with respect to the envelope can have physically observable effects. We can see in Fig 1.1 that for a many cycle pulse a phase offset of $\pi/2$ does not change the magnitude of the field appreciably, the maximum field strength of the shifted pulse is more than 99.5% of that of the un-shifted pulse, particularly near the maximum of the envelope, however for a few cycle pulse the same phase shift reduces the field magnitude by over 6% near the maximum of the envelope. If the CEP fluctuates randomly across all of 2π then it is obvious that CEP effects will not be observable in any experiment, which cannot observe interactions pulse by pulse. Since many experiments must acquire data over many pulses it is necessary to stabilize the CEP of a laser system in order to measure its effect on an interaction. For laser oscillators this can be done using the frequency comb self

referencing method[7]. In this method it is recognized that the pulsetrain from a laser oscillator is represented in the frequency domain by the overlap of a comb representing the cavity's allowed modes and the frequency response of the lasing medium

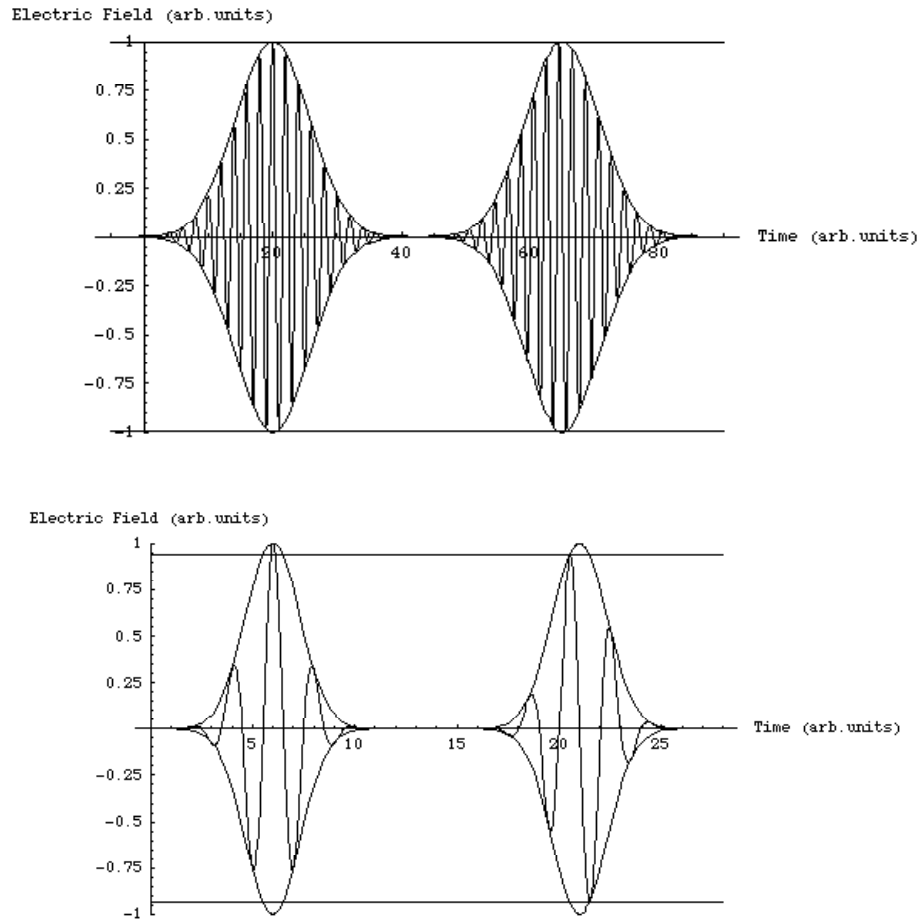


Fig 1.1

In the many-cycle pulses (top) a change of $\pi/2$ in the CE-Phase introduces very little discernable effect on the field strength an atom or molecule would feel. In the few-cycle pulses (bottom) the same $\pi/2$ CE-Phase shift produces a change in the maximum field strength near to 6%, which is significant for intense laser pulses in atoms or molecules.

A pulse-to-pulse shift of the frequency comb corresponds to a pulse-to-pulse shift of the CEP[7,8]. The offset frequency of the comb, the quantity that must be locked, is then

termed f_0 . In the self-referencing technique the spectral bandwidth of the laser is broadened using (SPM) such that for some frequency in the spectrum, f the spectrum also contains its second harmonic $2f$, this is a so-called octave spanning laser spectrum. By interfering these two frequencies it is possible to determine f_0 . Feedback control of the Kerr-Lens Mode-Locking (KLM) mechanism enables the fixing of f_0 such that it is a fixed fraction of the laser repetition rate f_{rep} , and thus locking the advance of the CEP[7,8]. A Pockel's cell can then be used to select pulses of the same absolute (but still unknown) CEP for amplification. Small feedback adjustment of the amplifier is then necessary to account for drift of the CEP introduced by the amplification[9-12]. This is done by implementing a second f to $2f$ interferometer, and using grating separation of the stretcher as the parameter for feedback control[10-13]. With this technique it is possible to control the CEP of the amplified pulses[10-13].

By combining this CEP stabilization technique with the hollow-core fiber compressor and a Ti:Sapphire amplifier it is possible to generate CEP stabilized few-cycle pulses. In this work we present the development of a Neon gas-filled hollow-core fiber compressor for the generation of CEP stable ~ 6 fs laser pulses with pulse energies >1 mJ. The matter of measuring this pulse duration must then be addressed. This is accomplished by the Frequency Resolved Optical Gating (FROG) method[14]. In this technique the laser pulse is split into two portions, which are interfered in a nonlinear medium. Spectral and temporal analysis of the resulting interferogram allow total pulse reconstruction.

The work described hitherto, however leaves the absolute CEP of the pulses unknown. As discussed before it is necessary to consider methods of measuring the

absolute CEP in atomic physics. Two physical phenomena have been demonstrated to be sensitive to the absolute CEP of a few-cycle laser pulse. These are threshold ionization (ATI) and high order harmonic generation (HHG)[15-18]. Therefore, in this work we present progress towards complete characterization of high energy few-cycle laser pulses using a phasemeter based on stereoscopic ATI and observations of evolution of HHG with CEP, both with Ar filled fibers.

Having traced the systematic generation, and characterization of these few-cycle, high-energy laser pulses, one will notice the large number of nonlinear processes at each step. In such circumstances it is quite intuitive that fluctuations in pulse energy will amplify at each nonlinear interface. Therefore stabilization of laser power is in fact a useful, and necessary endeavor. This technique may ultimately prove critical for proper characterization of the CEP lock of these few-cycle pulses.

In regards to the organization of this information it is presented as follows. In chapter 2 a brief overview of some topics related to the theory of SPM, the mechanism by which we generate our few cycle pulses will be presented. In chapter 3 the theory and experimental techniques of CEP locking will be discussed. In the first half of chapter 4, the experimental apparatus will be discussed. This consists of an explanation of the Kansas Light Source ultrafast Ti:Sapphire laser system, the hollow-core fiber compressor, and the power locking technique. In the second half of chapter 3 the characterization of the hollow-core fiber compressor output will be presented. There are four parameters to be discussed here: 1) The spatial mode quality 2) the pulse energy 3) the pulse duration 4) the CEP stability. In chapter 4 more specifics of ultrafast laser pulse measurement will be presented. This will be broken into two sections; the first section

focusing on autocorrelation, and the second focusing on the Frequency Resolved Optical Gating (FROG) method. Chapter 5 will address the use of HHG to determine the absolute CEP. In Chapter 6 conclusions and future work will be addressed. This will largely focus on methods of improving these results and work, which can proceed from whence this work ends. Topics include differential pumping of the hollow-core fiber to produce a gas pressure gradient, SPM in a filamentation chamber, and further HHG studies.

Chapter 2: Theory of Self Phase Modulation

2.1 The Nonlinear Propagation Equation

In 1967 it was observed that laser pulses of 10ps nominal duration from a pulsed ruby laser passing through a glass cell containing CS₂ were spectrally broadened by the medium [19]. This broadening is due to Self-Phase Modulation (SPM) the process by which an intense laser pulse's phase can be modified by its own presence in a medium. Thus the index of refraction, n can be expressed as

$$n = n_0 + n_2 I(t) \quad (2.1)$$

Where I is the laser intensity, n_0 is the linear refractive index and n_2 is, for a given frequency and medium a constant. If the polarization of a material under the influence of the laser field can be treated as a power series, as it can be in the perturbative regime in which we work, this coefficient is proportional to the third order susceptibility of the material[20,21]. This is in temporal analog to the Kerr lensing effect in which an intense laser-field alters the refractive index of a material creating an effective lens in the shape of the beam profile and focusing the beam as it propagates through the material. We can consider the effect of the laser pulse as introducing a nonlinear phase into the argument of the harmonic portion of the laser pulse. This is given as:

$$\phi_{nl} = -\frac{n_2 I(t) \omega_0 L}{c} \quad (2.2)$$

where L is the propagation length. This nonlinear phase clearly has a time dependence to it that is, in the form of the intensity profile, more complicated than linear. Since a frequency is essentially the derivative of a phase with respect to time this nonlinear

phase, and its non-zero temporal derivative implies the possibility additional frequency components beyond the initial spectral composition of the pulse:

$$\omega(t) = \dot{\Phi} = \omega_0 + \dot{\phi}_{nl} = \omega_0 + \frac{n_2 \omega_0 L}{c} \dot{I}(t) \quad (2.3)$$

where $\Phi(t)$ is the total phase. It is this time dependant frequency, which depends on the intensity of the laser pulse that enables the spectral broadening of the input pulse in the frequency domain.

We expect that a laser pulse's evolution in a medium is described by a partial differential equation. We also expect that the pulse's behavior can be fully described by Maxwell's equations. The propagation equation is referred to as the Nonlinear Schrödinger equation; it is obtained in most texts on nonlinear optics[20,21]. We can express Maxwell's equations in mks units, assuming a source-free medium

$$\begin{aligned} \nabla \cdot \vec{D} &= 0 & \nabla \times \vec{E} &= \frac{\partial \vec{B}}{\partial t} \\ \nabla \cdot \vec{B} &= 0 & \nabla \times \vec{H} &= \frac{\partial \vec{D}}{\partial t} \end{aligned} \quad (2.4a-2.4d)$$

The electric polarization of the medium, \vec{P} , is then given by

$$\vec{D} = \epsilon_0 \vec{E} + \vec{P} \quad (2.5)$$

By twice taking the curl of the electric field and exploiting the constituent relation we can obtain

$$\nabla \times \nabla \times \vec{E} = \frac{1}{c^2} \frac{\partial^2 \vec{E}}{\partial t^2} - \mu_0 \frac{\partial^2 \vec{P}}{\partial t^2} \quad (2.6)$$

By simple vector algebra and realizing that the gradient of the divergence of the electric field is almost always either negligibly small, or identically zero we can obtain the wave propagation equation

$$\nabla^2 \vec{E} - \frac{1}{c^2} \frac{\partial^2 \vec{E}}{\partial t^2} = \mu_0 \frac{\partial^2 \vec{P}}{\partial t^2} \quad (2.7)$$

If we then chose to express the polarization as the sum of a linear and nonlinear portion, $\vec{P} = \vec{P}_l + \vec{P}_{nl}$, we can rewrite this as

$$\nabla^2 \vec{E} - \frac{1}{c^2} \frac{\partial^2 \vec{E}}{\partial t^2} = \mu_0 \frac{\partial^2 \vec{P}_L}{\partial t^2} + \mu_0 \frac{\partial^2 \vec{P}_{NL}}{\partial t^2} \quad (2.8)$$

This nonlinear vector differential equation cannot be solved exactly. Therefore numerical solutions are required to determine the evolution of a laser pulse in a nonlinear medium, however the dimensionality of the equation makes direct numerical evaluation impractical as well. Therefore it is necessary to look for simplifying assumptions and approximations, which can yield an approximate form of the propagation equation, which can be, from a practical perspective, solved numerically. In fact we are not really interested in the behavior of the electric field as a function of three coordinate variables. From eq (1.2) we recall that we think of a laser pulse as a scalar amplitude in the propagation coordinates z and t . Thus an equation, which governs this amplitude is of interest. This leads to a family of nonlinear partial differential equations known as nonlinear Schrödinger equations, which can be obtained in various approximations from eq. (2.6). Obtaining such an equation is not the point of this work. One such equation of particular interest for the propagation of a laser pulse in a fiber compressor is given in[22]. Pulse propagation calculations are typically done in a retarded reference frame in which a retarded time T is defined as $T = t - z/v_g$. If the envelop of interest is $A(z, T)$, then $U(z, T) = A(z, T)/\sqrt{P_0}$, and the propagation equation is:

$$\frac{\partial U}{\partial z} + \frac{\alpha}{2} U + \frac{i}{2} \beta_2 \frac{\partial^2 U}{\partial T^2} - \frac{1}{6} \beta_3 \frac{\partial^3 U}{\partial T^3} = i\gamma P_0 \left[|U|^2 U + \frac{i}{\omega_0} \frac{\partial}{\partial T} (|U|^2 U) \right] \quad (2.9)$$

In which α is the loss coefficient, β_n is the nth order dispersion, and γ is the nonlinear parameter. It is then instructive to learn that the two terms on the right hand side govern SPM, and self steepening respectively. This equation is solved numerically in[22] by way of the split-step Fourier method[20]. In this method an initial envelope function is propagated by dividing the total propagation length into many small steps, then acting alternately with a dispersion operator and a nonlinear operator. It is important to recognize the basic theoretical groundwork associated with this work. From an experimental perspective comparison with results of this type will not be made, in no small part because of the difficulties involved in such comparisons. More direct comparisons with theoretical results can be made however, with the broadening factor to be discussed in the next section.

2.2 The Broadening Factor

We define the broadening factor of a gas-filled hollow-core fiber to be given as the ratio of the spectral width of the output pulse to the spectral width of the input pulse $F = \Delta\omega/(\Delta\omega)_0$. It has been shown that a simple expression for the broadening factor can be obtained in terms of the maximum phase shift, φ_m [15,16].

$$F = \left(1 + \frac{4}{3\sqrt{3}}\varphi_m^2\right)^{1/2} \quad (2.9)$$

The maximum phase shift can then be expressed as

$$\varphi_m = P_0 \frac{n_2 \omega_0}{c} \frac{L_{eff}}{A_{eff}} \quad (2.10)$$

Where P_0 is the peak power, n_2 is the nonlinear refractive index, c is the speed of light in vacuum, L_{eff} is an effective interaction length and A_{eff} is an effective modal area of the coupled beam in the fiber. The broadening factor has been calculated as both a function

of gas pressure and laser pulse duration for both Ar and He gas with input pulse energies of 1mJ and 5mJ respectively, the most noteworthy result for comparison to this work is that for input pulses of 25fs pulse duration and 1mJ energy coupled to Ar fiber a maximum broadening factor of approximately 5 was obtained[22]. However literature searches have yielded no similar calculation for Ne gas. Such calculations are severely limited by knowledge of the intensity dependent index of refraction for a given wavelength and pressure, let alone as a function of both[23]. Given this information the broadening factor can be estimated for a Neon fiber using (2.7). Calculations performed for this work using a value of $6 \times 10^{-25} \text{ m}^2/\text{W} \cdot \text{atm}$ [23], however yielded a broadening factor of approximately 12. This however must be taken purely as an estimate. A typical Ti:Sapphire amplifier with 40nm full-width at half maximum (FWHM) of bandwidth could be broadened to a maximum of nearly 500nm of bandwidth. The spectrum would be modulated, and thus FWHM would not be a particularly useful width definition. The spectrum would then most likely extend beyond the 500nm defined by a FWHM. It should therefore be noted that such spectral broadening is not useful, as chirp mirrors that support that kind of bandwidth do not currently exist. Thus, this calculation should serve only to provide some intuition that a Ne filled hollow-core fiber is capable of sufficient spectral broadening for our application.

Chapter 3: The Carrier-Envelope Phase Offset

3.1 Theory of the Carrier-Envelope Phase

Conceptually the Carrier-Envelope Phase Offset (CEP) is the best explained by expressing a laser pulse mathematically as a wavepacket composed of the product of some kind of envelope function (Gaussian, sech^2 , etc...) and a harmonic oscillating function:

$$\tilde{E}(z,t) = A(z,t)\exp(-i(k_0z - \omega_0t + \phi)) \tag{3.1}$$

In such a wavepacket as ϕ_{ce} is changed the wave will move with respect to the envelope. The CEP is the phase angle corresponding to the offset of the maximum of the wave that of the envelope. To reinforce this important concept Fig 1.1 is reproduced here:

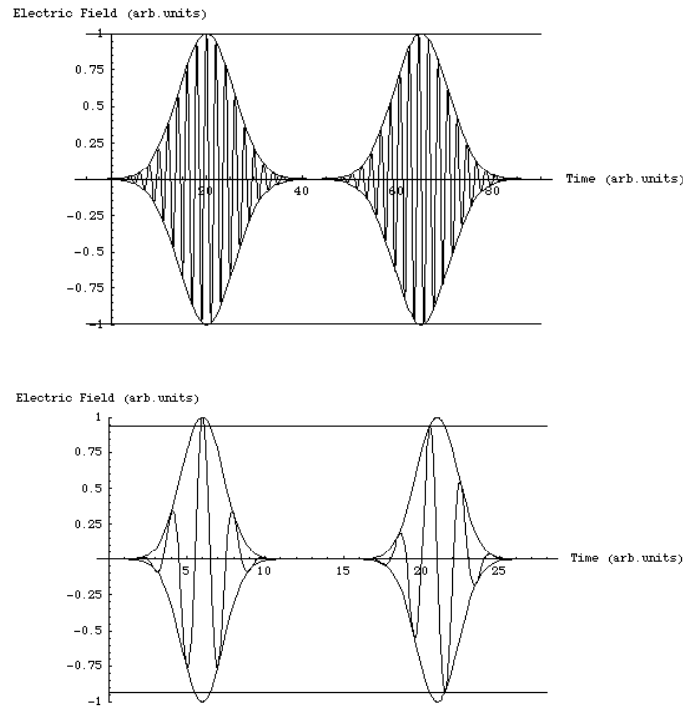


Fig 3.1.1

In the many-cycle pulses (top) a change of $\pi/2$ in the CE-Phase introduces very little discernable effect on the field strength an atom or molecule would feel. In the few-cycle pulses (bottom) the same $\pi/2$ CE-Phase shift produces a change in the maximum field strength near to 6%, which is significant for intense laser pulses in atoms or molecules.

A laser oscillator cavity generates a train of laser pulses by propagating a pulse back and forth between a highly efficient reflecting mirror and a slightly lower efficiency mirror that allows transmission of the pulse. The pulse is generated by coherent superposition of light waves. The uncertainty relation, a well-known consequence of wave mechanics, dictates that the shorter the laser pulse is the broader the distribution of spectral components that comprise it must be. To qualify as a laser this cavity then requires a lasing medium within the cavity and an external pumping source. Pumping in modern ultrafast laser oscillators is typically done with CW neodymium doped solid-state lasers, which are doubled to produce a few Watts of laser power in the green region of the spectrum[25]. Ti:Sapphire has become the mainstay of modern ultrafast laser oscillators and amplifiers as a lasing medium[26]. The wide band structure of Ti:Sapphire provides a source of broadband laser radiation, and thus a potential source of short pulses[26,27]. The laser cavity, however will not support all these laser frequencies. A laser cavity can be characterized, in part by, its frequency comb. This frequency comb is simply a series of peaks in the frequency domain corresponding to the frequencies supported by the cavity. The first peak corresponds to the fundamental frequency of the cavity, and the spacing is equal to the repetition rate of the laser. The former is given by:

$$f_{fundamental} = \frac{c}{nL} \quad (3.2)$$

where L is the cavity length. The later is given by:

$$f_{rep} = \frac{c}{2L} \quad (3.3)$$

It is therefore the overlap of the frequency response of the lasing medium, and the frequency comb of the laser cavity that determines the spectral composition of the output pulse. Fig 3.1.2 graphically summarizes the pulse train represented in the frequency domain.

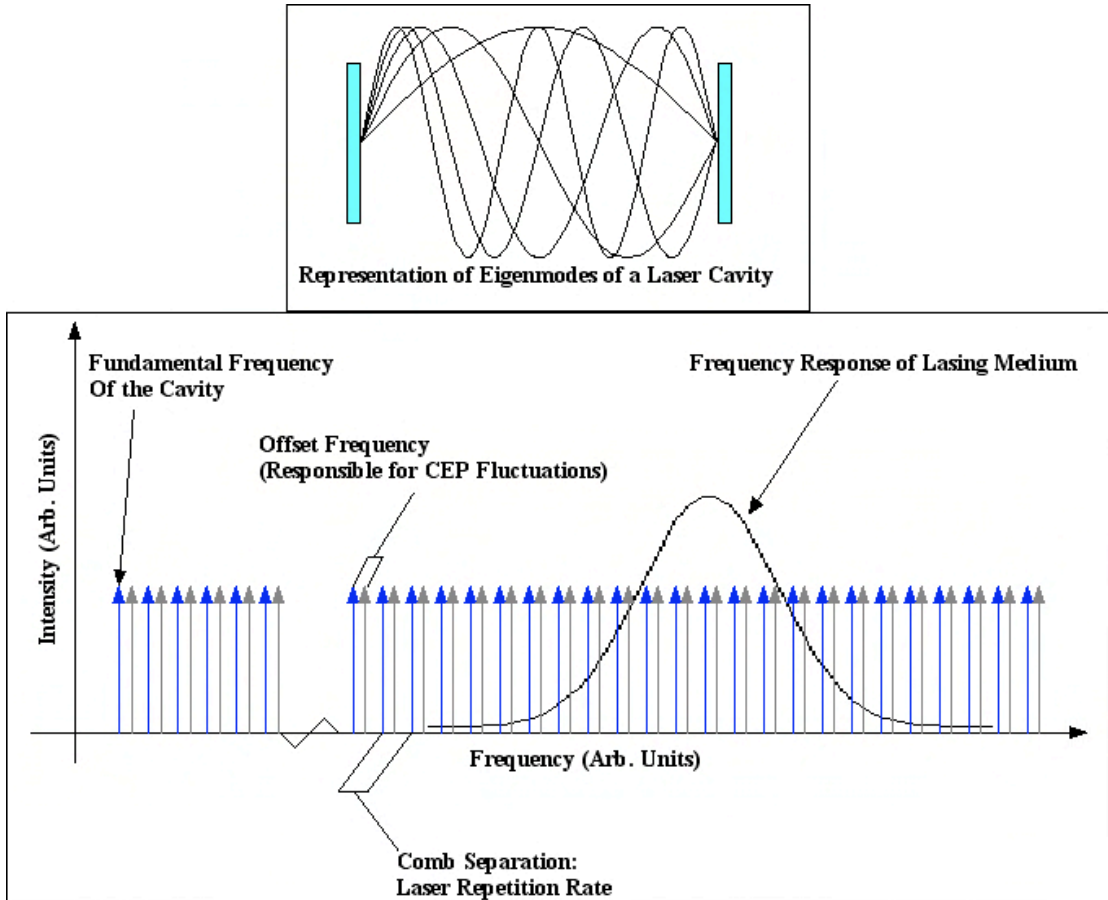


Fig 3.1.2

The modes supported by the cavity are represented both in the time domain (top) and frequency domain (bottom). The cavity modes form a comb in the frequency domain, with teeth separated by f_{rep} . This comb, coupled with the frequency response of the lasing medium enable short pulse generation. Shifting of the frequency comb by some offset frequency f_0 will result in pulse to pulse changes of the CEP.

The criterion stated above, that the superposition be coherent cannot be understated. A direct phase relation of all the spectral components is required for short

pulse generation. Fig 3.1.3 shows the superposition of twenty equally weighted eigenmodes of a cavity with random phases and with the same phase. It can be clearly seen that the random phase case results in apparently random noise, while the case in which the phases are equal results in a pulsetrain. Locking the phase of the temporal modes of a cavity for short pulse generation is termed mode-locking, and is requisite for short pulse generation. Mode-locking is accomplished by introducing a fast saturable absorber into the laser cavity. The fast saturable absorber will, as its name implies, absorb laser energy until it saturates. Thus it passes the highest intensity portion of a pulse while absorbing lower intensities at the wings, thus steepening the pulse. It is known that the Kerr-Lens effect in Ti:Sapphire acts as a fast saturable absorber, thus enabling mode locking without a separate element in the cavity[28]. This is Kerr Lens Mode-locking (KLM). All work described herein was done with a KLM oscillator.

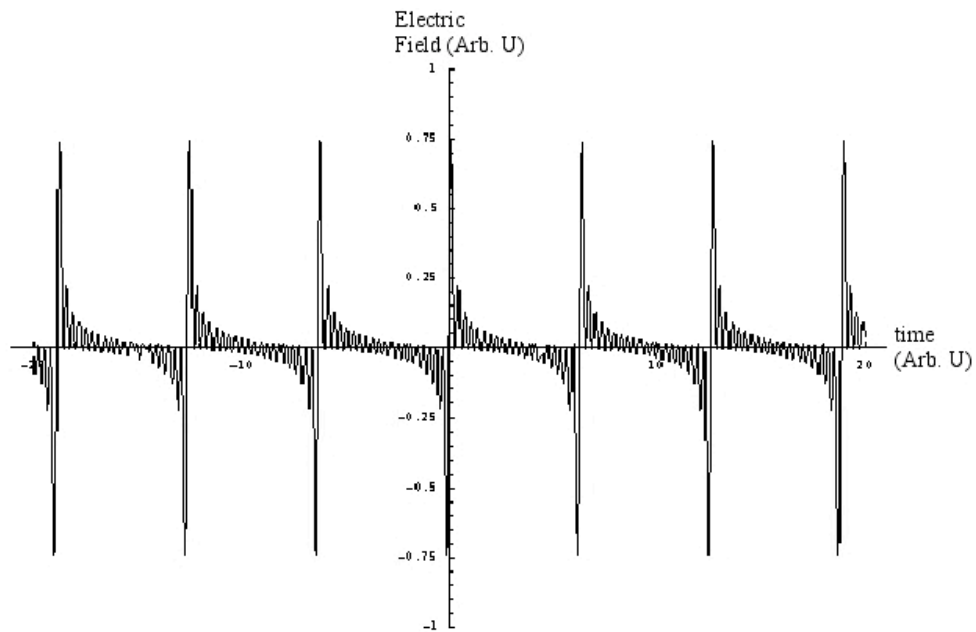
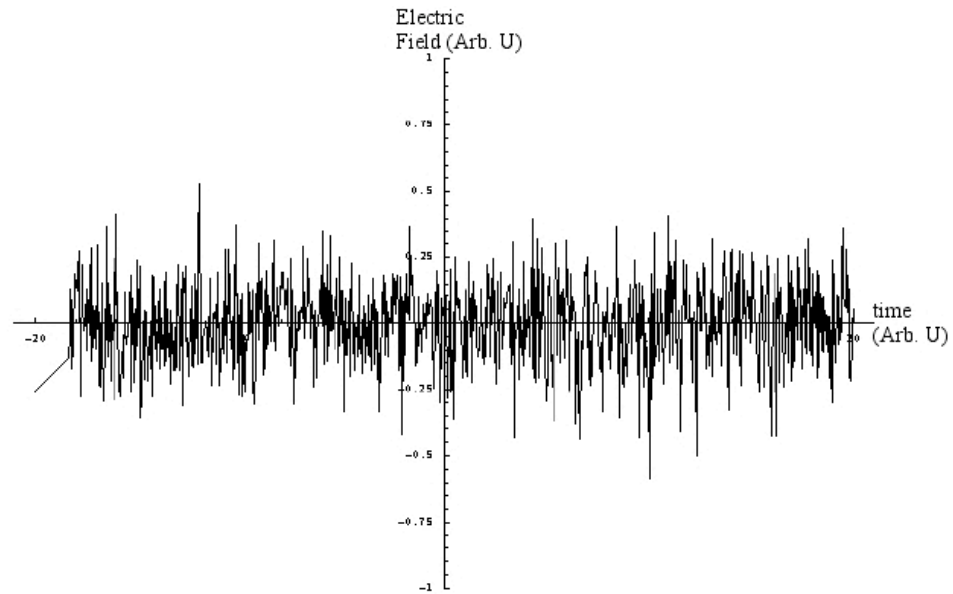


Fig 3.1.3

The equally weighted superposition of twenty simple eigenmodes of a perfectly reflecting cavity are shown in both graphics. In the topmost image the spectral components share a random phase. In the lower image they have the same phase. This is the essence of mode-locking a laser for pulse generation.

Having generated short pulses within the laser cavity we should note that the cavity contains dispersive media in the form of air and the lasing medium, and in these

media the group and phase velocities, will of course differ by some small amount. Thus the carrier wave will move with respect to the envelope as the pulse propagates within the cavity, and whatever phase the carrier-wave has with respect to the envelope when the pulse reflects off the 90% reflectance mirror, will determine the absolute CEP of the pulse exiting the laser cavity.

It is intuitive that if every time the pulse propagating within the cavity made a roundtrip the pathlength and amount of material were exactly the same each pulse would have the same absolute CEP. However vibrations of the cavity, temperature changes, and air currents can all change either the path length, the amount of material in the laser path, or both. As mentioned before, there are experiments that are sensitive to the absolute CEP of a few-cycle laser pulse, and it is therefore necessary to address a method of locking the CEP. It has been shown that pulse to pulse fluctuations of the CEP in the time domain correspond to a fixed shift of the cavity comb in the frequency domain[7,8]. Furthermore changes in the cavity length represent stretching or compressing the comb, as this change results in a change to f_{rep} , which is the comb spacing. We can see that locking the advance of the CEP can be expressed as the problem of locking the shift of the frequency comb, and that if we can somehow lock it to a multiple of f_{rep} the system is then immune to stretching of the comb, as that change will be self-correcting.

3.2 CEP Locking Apparatus for the KLS Oscillator

From a practical standpoint the locking of the CEP of pulses from a mode-locked Ti:Sapphire laser has already been reduced to locking the frequency comb, using the repetition rate as a reference. Furthermore it seems intuitive that the way to do this might be to tune the cavity dispersion; this intuitive approach will prove to be a quite accurate

description of what is done. First, however it is necessary to construct a mechanism by which we can measure the offset frequency, f_0 .

This is done via the self-referencing method of f to $2f$ interferometry. If the laser pulse spectrum is sufficiently broad that it spans from a frequency f to $2f$ (where “spans these two frequencies” is given to mean “has measurably useful intensity at these two frequencies”) then the frequency comb associated with this pulse will overlap with that of the pulse generated through SHG. The implications are significant. Since the SHG process, does not double the frequency of an electromagnetic wave, so much as it doubles the entire phase, beating a frequency in the short wavelength portion of a pulse with the same frequency in the low frequency end of the doubled pulse gives the carrier-envelope offset frequency. This is done in a Mach-Zehnder f to $2f$ interferometer with a nonlinear crystal in one of the arms. The beat frequency is extracted by first spatially separating the light with a grating, filtering it with an aperture and finally using an avalanche photodiode and electronic signal processing for final detection. In the KLS system, SHG for this purpose has previously been done with BBO, though currently a periodically poled KTP crystal is used for increased SHG yield.

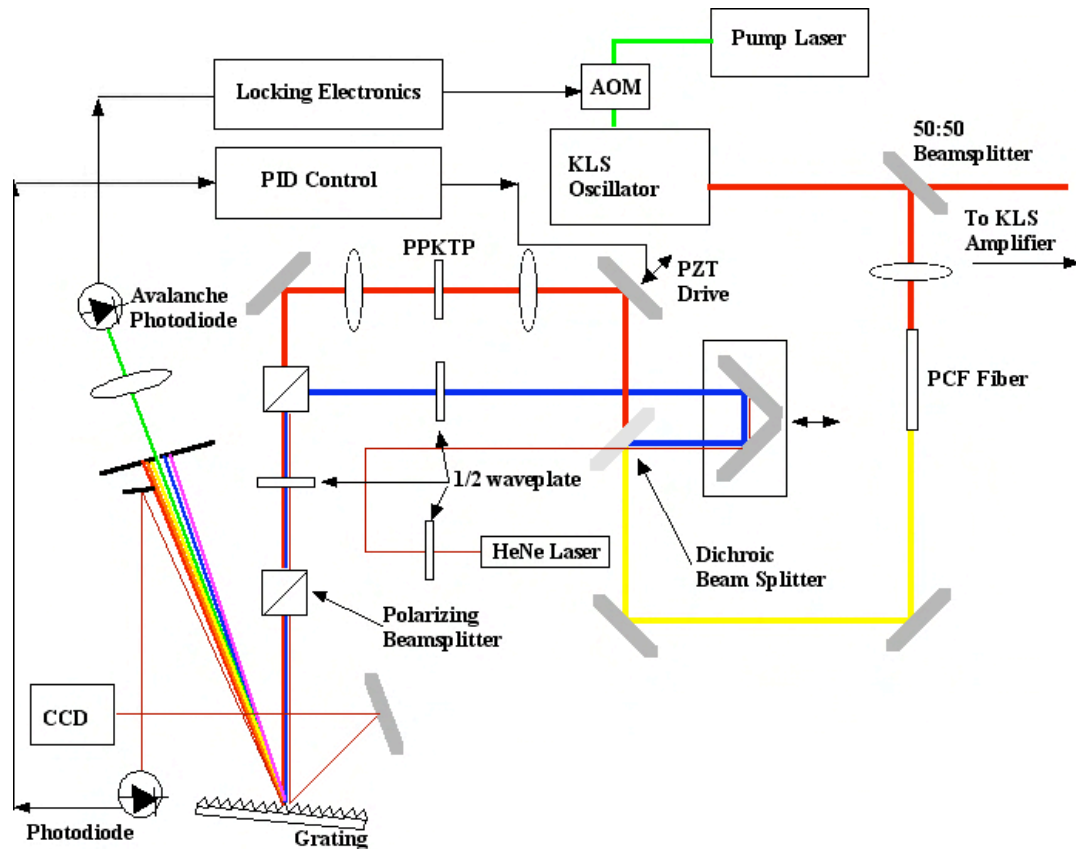


Fig 3.2.1

The CEP stabilization system for the KLS oscillator centers around a Mach Zehnder f to $2f$ interferometer. The nonlinear medium is periodically polled KTP. A HeNe laser can be used to feedback to a PZT for additional interferometric stability.

Having measured the offset frequency, it can be locked by measuring its drift (phase noise) electronically, and then feeding back to control the dispersion of the cavity. The feedback parameter is the KLM. An Acousto-Optica Modulator (AOM) is used to finely control the pump power input into the oscillator. This, naturally affects the Kerr lens, and modifies the dispersion experienced by the pulse within the cavity.

3.3 Feedback Correction of the CEP Drift in the KLS Amplifier

CEP stabilized pulses passing through an amplifier will have their CEP affected by the amplification process. At the most basic level this is again understood by looking at the dispersive media (air, glass, Ti:Sapphire, etc...), and once again each pulse cannot

be assumed to be affected in the same way. Air currents, vibrations, temperature changes, and other largely uncontrollable fluctuations make certain the total phase delay accrued by each pulse is different. However if an experiment requires the fixing of the CEP it is important to control the CEP through the amplifier as well. It is therefore necessary to discuss methods of quantifying the CEP drift through the amplifier causes of this CEP drift and methods of correcting it.

To quantify the CEP drift through the amplifier, again the method of f -to- $2f$ interferometry is used. In this case the amplified laser pulses are spectrally broadened using filamentation in a sapphire plate and then passed through a collinear f -to- $2f$ interferometer, as depicted in Fig 3.3.1. Now, however the repetition rate of the laser is 1kHz, and there isn't really a laser cavity to speak of. Therefore there really isn't a frequency comb, and if there were, the comb spacing would be inconveniently small. Thus locking an offset frequency associated with a frequency comb is not a useful picture for correcting the CEP through the amplification process. Instead it is useful to consider that a phase delay between two pulses in the time domain will generate interference fringes in the frequency domain. To this end the spectrally broadened pulses are passed through a nonlinear medium, a BBO crystal, for SHG. The doubled pulse will, as a result of the fact that both the group and phase velocities in the Sapphire and BBO crystal are functions of frequency, experience both group and phase delays, with respect to each other.

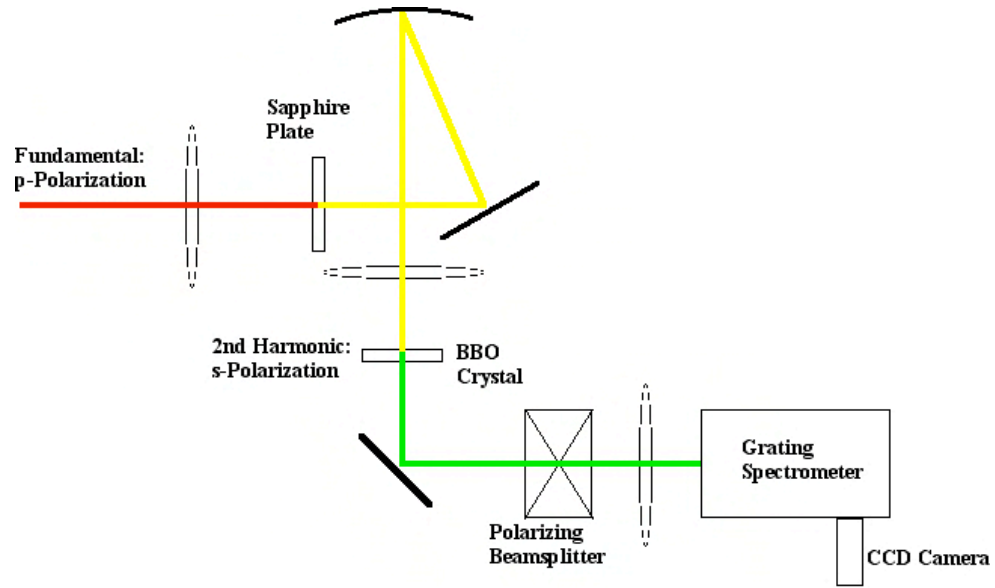


Fig 3.3.1

The collinear f -to- $2f$ interferometer design that is used for measuring the phase drift through the KLS amplifier.

The sapphire plate both spectrally broadens the pulse, and also chirps it, such that the red portion of the pulse leads the blue portion. The BBO crystal will then produce a pulse that is also chirped, but also slightly separated from the fundamental pulse in time, such that the $2f$ portion of the SHG pulse overlaps with the $2f$ portion of the original pulse. Again, a cube polarizer is used to heterodyne these two waves. The interferogram in the frequency domain is observed with a grating spectrometer and CCD camera. A shift in this interference pattern of one fringe corresponds to a CEP shift of 2π .

Correction of the CEP drift through a CPA amplifier translates to locking the interferogram. In this work this is done by feedback control of the grating separation in the stretcher or compressor (for CPA systems with grating based stretchers/compressors)[]. The CEP drift through the amplifier can be broken down essentially into two components, a fast variation which has frequency components up to

1kHz, the repletion rate of the amplifier, and a slow component that acts over multiples of seconds.

The f to $2f$ interferometer and feedback control loop are inextricably tied together. This has implications for the measurement of the CEP stability made with this interferometer. In fact the feedback loop does not correct the CEP of the pulse, alone. The feedback loop is designed to keep the fringes of the interferogram fixed in the frequency domain. Thus the feedback loop compensates for anything that introduces drift in these fringes, even if such a mechanism doesn't really affect the CEP. This can result in a feedback loop, which rather than correcting the CEP steers it in ways which are undesirable. Since changes in the laser power will be amplified in magnitude by the filamentation process in the sapphire plate and these changes will shift the fringes, there is at least one mechanism of this type. To help remedy this situation a second f to $2f$ interferometer is used to measure the CEP independently. We term the first f to $2f$ measurement the inloop measurement, and the second the outloop measurement.

Chapter 4: The Hollow-Core Fiber Compressor Experiment

4.1 Experimental Apparatus

4.1.1 The Kansas Light Source Laser System

All experiments described in this thesis were completed using the Kansas Light Source Laser System (KLS), it is therefore valuable to discuss, this laser system in some detail. The KLS consists of a mode-locked Ti:Sapphire oscillator and a single-stage multi-pass Ti:Sapphire CPA amplifier. The KLS is shown in Fig 4.1.1.1.

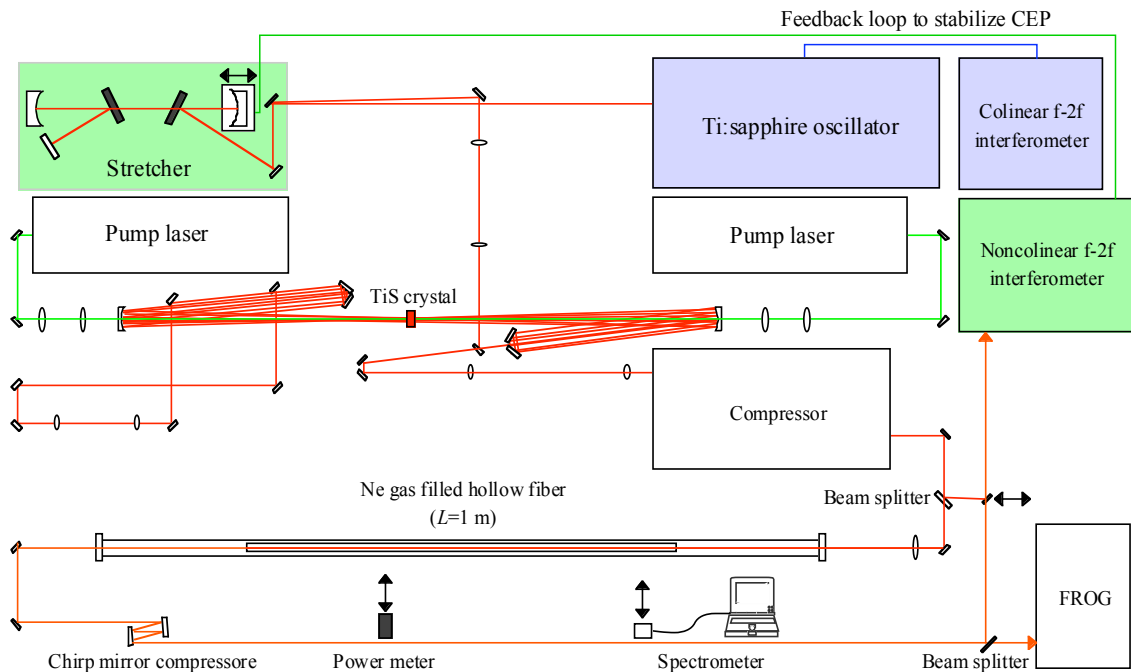


Fig 4.1.1.1

The Kansas Light Source Laser System is a Ti:Sapphire Oscillator and Amplifier system with CE-Phase locking capabilities, fiber compressors for few-cycle pulse generation and diagnostics for measuring CE-Phase stability (f -to- $2f$ interferometers) and pulse duration (FROG).

The oscillator is pumped by ~ 4 W (continuous wave) of 532nm light and has a repetition rate of ~ 77 MHz, producing 12fs pulses of 2.6nJ energy. From this pulsetrain a Pockel's

cell selects pulses at a 1kHz rate. These pulses are then stretched in time via a grating pair in a positive dispersion configuration to ~ 80 ps. They are then amplified by 14 passes through a liquid nitrogen cooled Ti:Sapphire crystal, which is longitudinally pumped by ~ 30 W of doubled Nd:YLF laser light (527nm) pulsed at 1kHz (~ 209 ns pulse duration). A second Pockel's cell placed after the seventh pass together with a change in focus volume serves to reduce amplified spontaneous emission (ASE). The 2.6nJ pulses are thereby amplified to almost 5mJ of energy. The amplified pulses are then recompressed via a negative dispersion grating pair, with an energy efficiency of approximately 50%. The result is a train of nominally 25fs pulses with energies up to 2.5mJ at a 1kHz repetition rate.

4.1.2 The Hollow-Core Fiber Compressor

The experimental set-up of a gas-filled hollow-core fiber compressor is shown in Fig 4.1.2.1. This setup consists mainly of a hollow glass waveguide (hollow-core fiber), approximately 0.9m long, of 6mm diameter and having a $400\mu\text{m}$ diameter hole along the longitudinal axis. This waveguide is mounted in a stainless steel tube of 25mm nominal diameter with 1mm thick windows attached on each end. The windows are reinforced with viton o-rings and brass plates. The windows are coated with an anti-reflection coating to reduce losses at the entrance and exit. The pressure within the chamber can be varied from under 70 μBar to over 4 Bars. The amplified laser beam from the KLS laser source is focused into the chamber where it is coupled to the hollow-core fiber. For this purpose the gas chamber is mounted on two sets of two dimensional translation stages which allows for very sensitive tuning of the fiber's height, transverse position, and tilt (in these two directions) relative to the beam. The output is then collimated using a

concave spherical mirror of 1.5m focal length. This collimated beam is then passed into a chirp mirror dispersion compensator set capable of providing the $\sim 300\text{-}400\text{fs}^2$ of group velocity dispersion necessary to compress the pulse below 10fs. After the chirp mirrors a pair of wedge shaped fused silica plates, or glass blanks can be inserted to further tune the dispersion of the pulses.

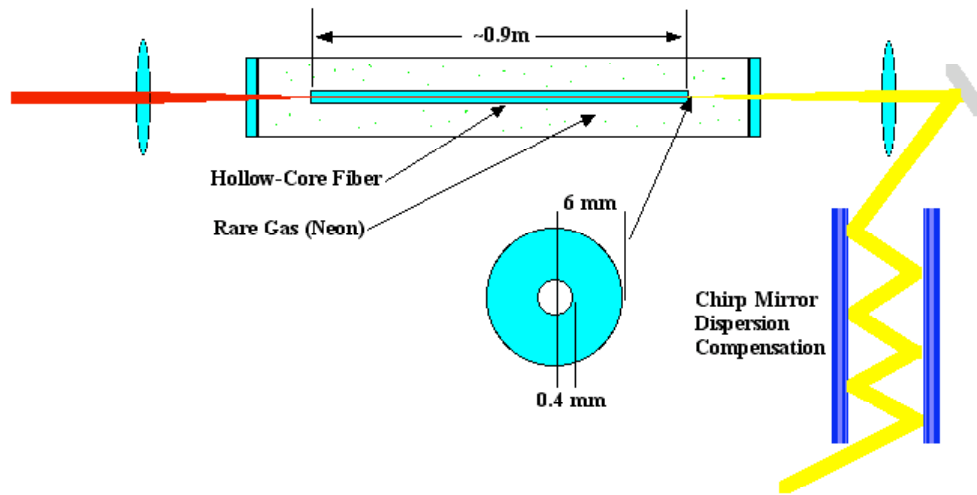


Fig 4.1.2.1

Schematic view of the hollow-core fiber compressor. Pulses of 25fs nominal duration are focused into a hollow glass waveguide slightly less than a meter in length containing a rare gas. Thus the pulse is spectrally broadened via SPM in the gas. After the fiber the spectrally broadened beam is collimated and the pulse compressed via chirp mirrors.

4.1.3 Stabilization of the KLS Laser Power

An important development in the KLS laser system is the addition of a feedback control system to stabilize power. This system again consists of an inloop and outloop measurement. A power meter using a photodiode sensing element is placed in position to observe the zeroth order diffraction from one of the gratings in the compressor, a beam which was previously wasted. This power meter feeds back into the voltage of the first Pockel's cell that picks pulses from the oscillator pulsetrain for amplification. Control of

this parameter can be used to stabilize the output power. A second power meter independently verifies the stability with and without the feedback control. The relationship between the CEP control in the KLS amplifier and the KLS power fluctuations is, at this point, still being actively studied experimentally. Data to be presented in section 4.2.4 suggests that power stabilization is beneficial to CEP stability if not critical.

4.2 Beam Characterization

To determine the effectiveness of the hollow-core fiber compressor it is necessary to characterize the output beam. In particular we are concerned with three parameters. We are first concerned with the coupling efficiency and mode quality of the output compared to the input beam. We are next concerned with the spectrum of the output beam. The last, and most important parameter, which we need to characterize is the duration of our pulse after necessary chirp mirrors and compensation plates.

4.2.1 Coupling Efficiency and Mode Quality

In order to produce a useful beam it is important to have maximum coupling efficiency from the hollow-core fiber compressor as well as a uniform beam profile. Clearly absorption in the gas will reduce the coupling efficiency. The fiber used in this work regularly yielded coupling efficiencies of ~85% when the chamber was pumped down to approximately 50mTorr and laser power was low and as high as 65% with ~3-4 Bars of Neon and maximum available power was coupled(~1.8mJ) near the theoretical limit[29]. Fig 4.2.1.1 shows a scan of output power as a function of input power taken with 2.3 bar of Neon in the fiber.

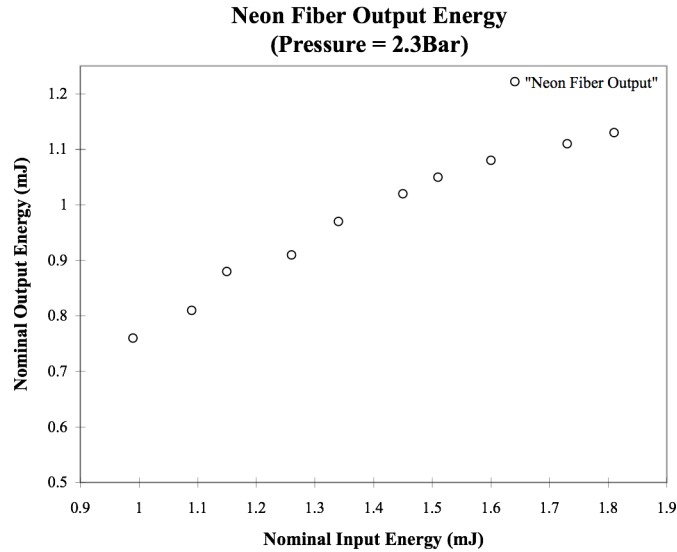


Fig 4.2.1.1

The output energy from a neon-filled hollow-core fiber is measured as a function of input energy. The gas pressure is ~2.3bar. Pulses with energy greater than 1mJ are clearly feasible for input pulses of approximately 1.8mJ

Although power limitations at the time that this data was taken prevented obtaining information for higher powers, it is clear from this data alone that pulses with 1mJ of energy are obtainable from a Neon fiber. Thus coupling pulses of nominally 1.8mJ energy to the neon fiber filled to 2.3bar of pressure can yield nearly 1.2mJ pulses spectrally broadened to nearly 350 nm of bandwidth.

The input beam is lightly focused via a 1.5m focusing lens for maximum coupling efficiency at the 400 μ m opening. Measurement of the input focus profile showed a uniform distribution of ~150 μ m spot size. The focusing lens was positioned on a translation stage with 25mm of translation available for fine-tuning the coupling. Translation of the lens showed the fiber coupling efficiency and mode quality to be relatively insensitive to this parameter. The fiber should yield a beam profile well-

represented by a zero order Bessel beam. For the sake of comparison to an ideal we compare this to a Gaussian beam with a spot size given by:

$$w(z) = w_0 \sqrt{1 + \left(\frac{z}{z_R}\right)^2} = w_0 \sqrt{1 + \left(\frac{\pi \omega^2}{M^2 \lambda z}\right)^2} \quad (4.1)$$

Where z_R is the Rayleigh range of the laser beam, and z is the propagation coordinate, or w_0 is the beam waist and M^2 is the beam quality factor. This beam quality factor is obtained by focusing the laser beam and performing a z-scan to measure

$$M^2 = \frac{w_0 \theta_{1/2}}{w_{0G} \theta_{1/2G}} \quad (4.2)$$

Where $\theta_{1/2}$ is the half angle beam divergence measured in the far field. The denominator contains the same parameters for an ideal Gaussian beam of the same wavelength. The z-scan would give $M^2=1$ in the ideal case. A z-scan was performed after the hollow-core fiber, with the beam focused by a concave mirror with 750mm focal length. The right panel of Fig 4.2.2.1 shows the spot size as a function of distance in the longitudinal direction for the output from the Neon-filled hollow-core fiber. An M^2 value of 1.08 was measured. The left panel of Fig 4.2.2.1 shows the spatial profile of the beam at the focus, yielding a spot size of 87 μm . The calculated diffraction limit is 75 μm . Thus we are certain that the hollow-core fiber yields a beam of good spatial profile, and mode quality. Although this is not our principle interest, it is an important characterization of our output.

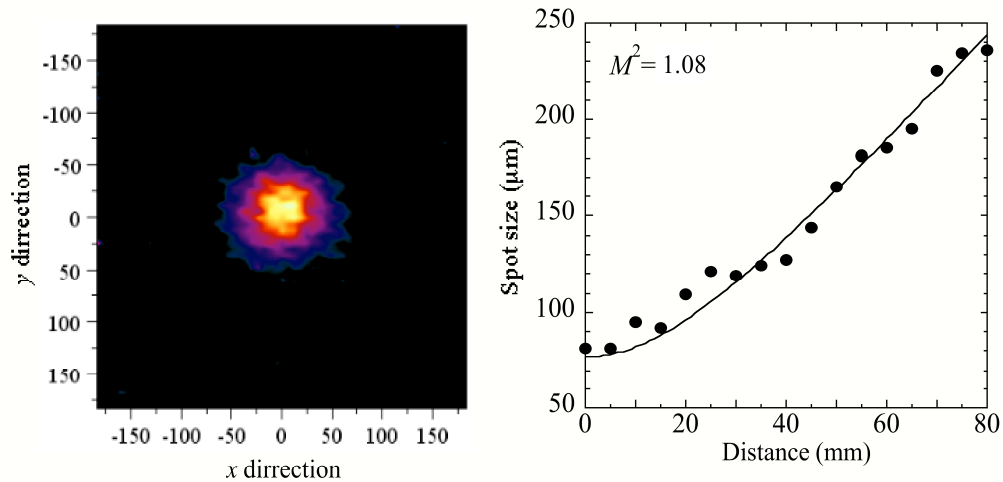


Fig 4.2.2.1

The focus spot size is measured and the beam profile is longitudinally scanned. From this data the M^2 is measured. We can compare this to an ideal M^2 value of 1.

4.2.2 Spectral Broadening

As noted previously we can define the broadening factor as the ratio of the spectral width of the output pulse to that of the input pulse. The spectrum of a laser can be measured with a simple grating spectrometer. In this work the spectrum of the beam was measured after propagating through the neon-filled hollow core fiber as both the pressure of the gas was varied. Data was taken with pulses of ~ 1.6 - 1.8 mJ of energy. It is worth recalling that since in the hollow-core fiber the spectrum is broadened by SPM, an effect of the intensity-dependant refractive index, thus in addition to pulse energy, the input pulse duration is a key parameter. Thus for day-to-day operation the grating compressor of the KLS was tuned (and thus the pulse duration was tuned) for optimal spectral broadening.

Quantifying the spectral broadening effect of the rare gas is made slightly difficult by the modulation of the spectrum characteristic of SPM. Normal criteria used for specifying the width of a peak, such as full width at half max, $1/e$, and $1/e^2$ width begin to lose their meaning as the spectrum becomes more of a broad, and modulated continuum, than a peak. Thus to the end of roughly quantifying the effect of gas pressure on the spectrum a course method of estimating the width of the spectrum is used. In this method the spectrum is examined on a logarithmic scale. The signal to noise ratio of a grating spectrometer exposed to scattered light from an intense laser is actually quite high, thus on the logarithmic scale it becomes possible to estimate the point in the spectrum where the laser spectrum is no longer detectable and only the background is contributing. Thus a full spectral width can be estimated. This can be seen clearly in Fig 4.2.2.1.

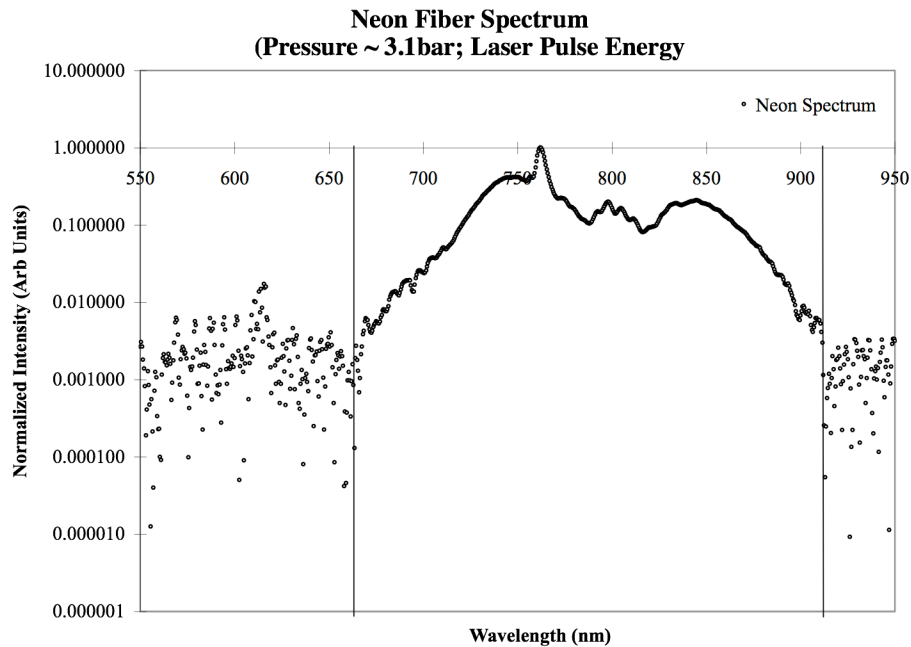


Fig 4.2.2.2

The favorable signal to noise ratio obtained when using a spectrometer to measure a laser spectrum enables an accurate estimation of a full-width, the width at which the spectrum cannot be discerned from the background. This concept is useful for quantifying the broadening of the spectrum with power, pressure or other parameters.

Using this concept of full width it is then clear from Fig 4.2.2.3 that spectral broadening increases with pressure.

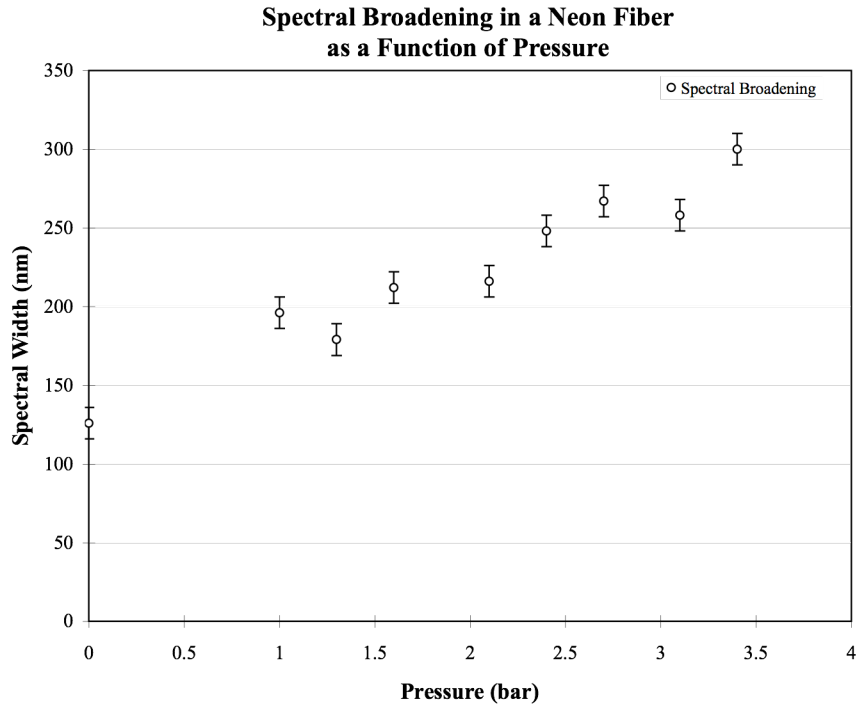


Fig 4.2.2.3

Spectral broadening of the KLS beam in the neon-filled hollow-core fiber as a function of gas pressure. Spectral broadening beyond 300nm can be achieved with pressures around 3-4 bar.

Varying the input energy showed a less quantifiable increase, as well, though at some point plasma defocusing will begin to dominate and the spectral broadening effect will saturate. Ultimately, however the chirp mirror compensation sets limits on how much spectral broadening is useful. The chirp mirrors can support a bandwidth, which spans nominally from 600-1000nm, and thus further broadening serves only to introduce loss, which is undesirable. An optimized spectrum is shown in Fig 4.2.2.4 with the spectrum of the KLS amplifier (which remains very constant from day to day).

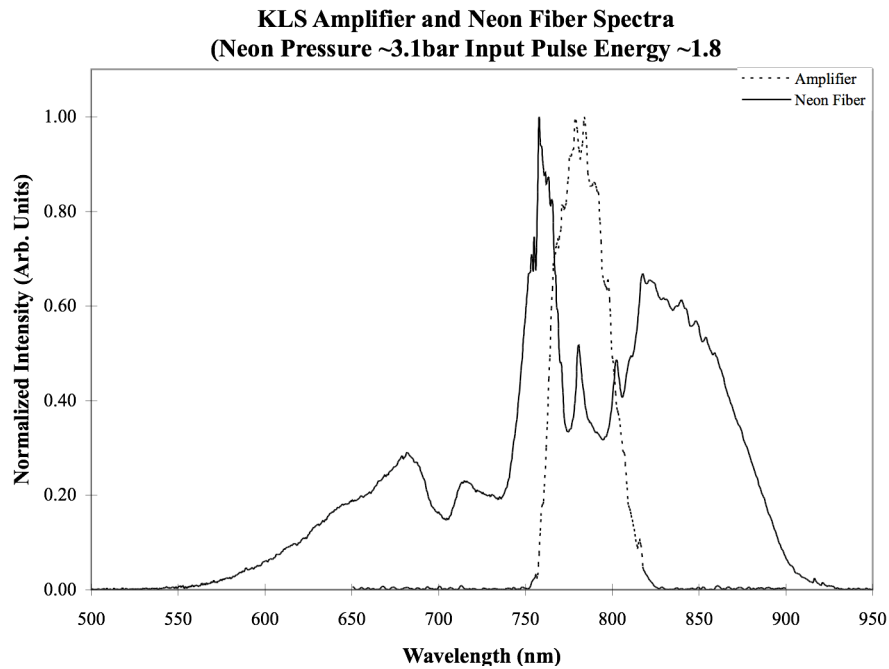


Fig 4.2.2.4

Optimized spectrum from the Neon filled hollow-core fiber compressor shown with the KLS amplifier spectrum. The output spectrum is broadened by a factor of 4.6

The fiber output is approximately 410nm full width compared to the KLS amplifier, which has a full width of 90nm, thus yielding a broadening factor of 4.6 similar to the maximum broadening factor numerically obtained for Ar fibers with 25fs input pulses, with significantly less output pulse energy[22].

4.2.3 Pulse Duration

There are three principle methods for measuring the pulse duration of an ultrafast laser pulse. These are autocorrelation[19,20], FROG[15], and Spectral Interferometry for Direct Electric Field Reconstruction (SPIDER)[22]. SPIDER, a form of shear spectroscopy, though having advantages over autocorrelation, is from a technical standpoint more difficult to implement, and is not used in KLS. As such, although it is important to recognize its existence, it will not be discussed at any further length. The

Kansas Light Source laboratory has the capabilities of measuring pulse duration via autocorrelation and SHG FROG, both of which will be discussed in more detail in chapter 5. FROG has advantages over autocorrelation, which will be discussed in chapter 5, making it a superior choice for pulse measurement. In a FROG measurement the pulse is measured in the two dimensional time-frequency domain, and its spectrogram is reconstructed via the FROG algorithm. Thus the agreement of the measured and recovered FROG trace is a good initial criterion for the quality of the pulse measurement. On top of this the FROG error should be minimized. The last thing which was sought for this pulse measurement was agreement between the autocorrelation and SHG spectrum calculated from the experimental and reconstructed FROG traces. With the neon fiber used in this work pulse durations of less than 8fs were demonstrated. A minimum pulse duration of 6.5 fs was measured via SHG FROG as shown in Fig 4.2.3.1, with a FROG error of 0.017. This can be compared with a transform limited pulse duration obtained from the Fourier transform of the pulse. The spectrum shown in Fig 4.2.2.2 has a transform limited pulse duration of 4.8fs full width half maximum, indicating that further compression should be possible. The figure shows the experimental and reconstructed FROG traces which are symmetric, as FROG demands, and in relatively good agreement as to shape and size. The figure also shows the autocorrelation and SHG spectrum from the two traces, and which both agree reasonably well. Thus as a first measurement this suggests already that a few cycle pulse of 1mJ energy has been achieved.

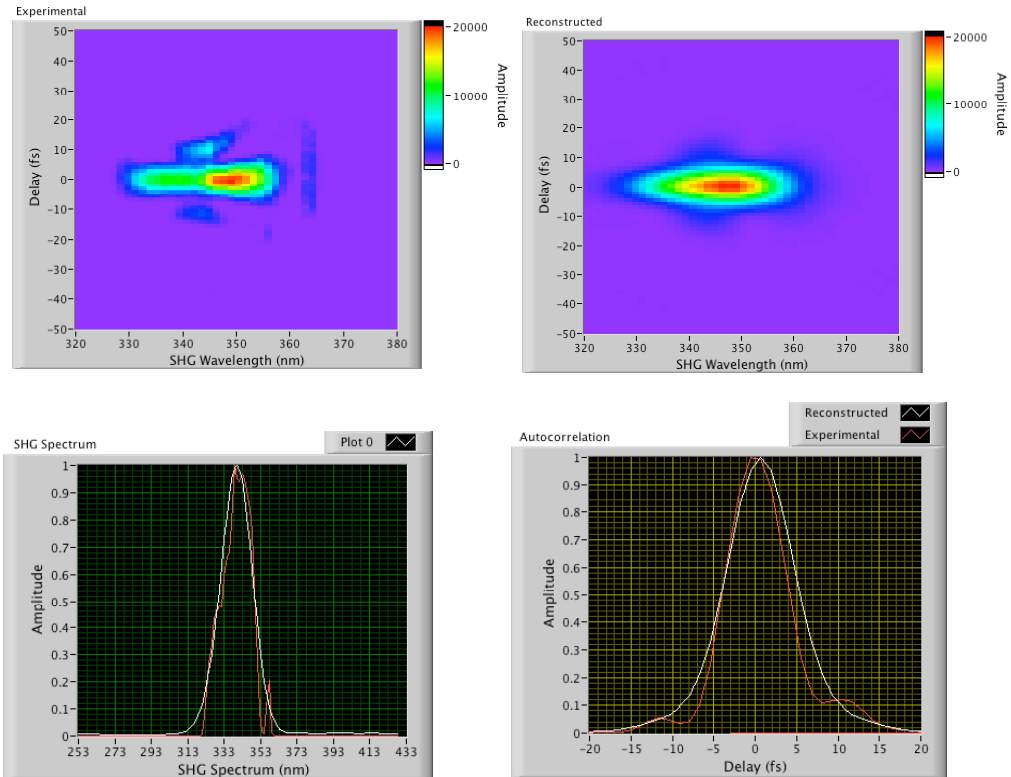


Fig 4.2.3.1a

The neon fiber output is compressed and measured by FROG the experimental FROG (top left) and reconstructed (top right), the agreement is good as a first measurement. The SHG spectrum and attocorrelation is compared for the experimental and retrieved pulse as well. The agreement is good at a gross level, but fine features have been lost. More refined measurements should be performed.

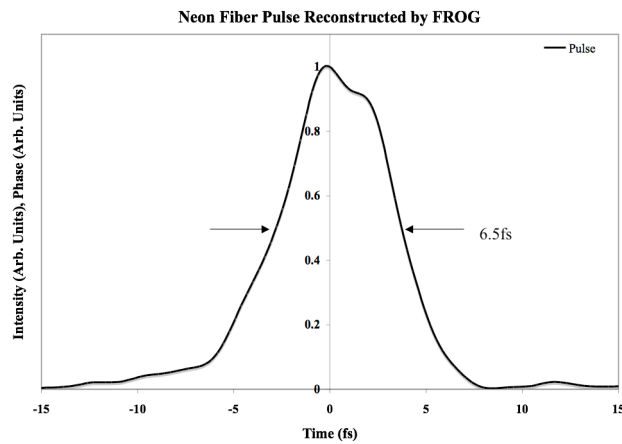


Fig 4.2.3.1b

The reconstructed pulse is then shown above yielding a pulse duration measurement of 6.5fs. This can be compared with a transform limit of approximately 4.9fs, indicating more compression should be feasible.

4.2.4 Carrier Envelope Phase Drift

The last parameter critical to our pulse characterization is the CEP stability. The methods of stabilizing the CEP of an oscillator, and amplifier have been discussed in some detail previously.

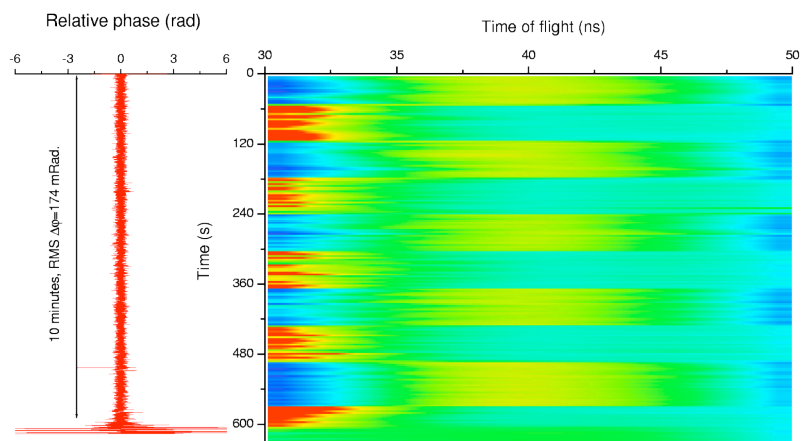


Fig 4.2.4.1

Count rate asymmetry in a stereoscopic CEP phasemeter showed CEP stability of an Argon filled hollow-core fiber compressor[10]. Changes in relative field strength associated with CEP changes result in count rate anisotropy. In this case the CEP was suddenly changed periodically using glass wedge plates.

CEP stabilization of an Ar fiber has previously been demonstrated via a CE-phasemeter based on stereoscopic ATI(see Fig. 4.2.4.1)[13]. In ATI photoelectrons are generated when the electric field of the laser field relaxes the atomic potential to the point where the electron wavepacket can tunnel to a free particle state. At that point the electron moves almost entirely under the influence of the electric field. It is then clear that the electrons will be emitted in the directions parallel to the laser polarization. A change in the CE-phase will result in a relative change of field strength between two adjacent half cycles.

Since the ATI process is sensitive to the electric field strength this will result in an anisotropy in ATI photoelectron countrate, which can be used as a measure of the absolute CE-phase, to within the natural 2π ambiguity.

In this section we will focus on first measurements of the CEP stability of this Neon fiber. In this experiment the CEP of the KLS oscillator was locked as usual. The slow drift of the amplifier was corrected using the collinear f to $2f$ interferometer technique. 10% of the amplified laser beam was directed to this set-up. The remaining 90% was coupled to the neon fiber. The fiber output was then directed to a second f to $2f$ interferometer to measure the CEP stability. Spatial filters and bandpass filters were used to eliminate additional interference beyond the desired f -to- $2f$. At the time of this data, feedback control of the laser power was not yet available, so this data is taken with no power feedback control. The CEP was locked and an RMS deviation of 487mrad was obtained over 3minutes. The CEP of the amplified laser pulse during that same period had a RMS deviation of 117mrad.

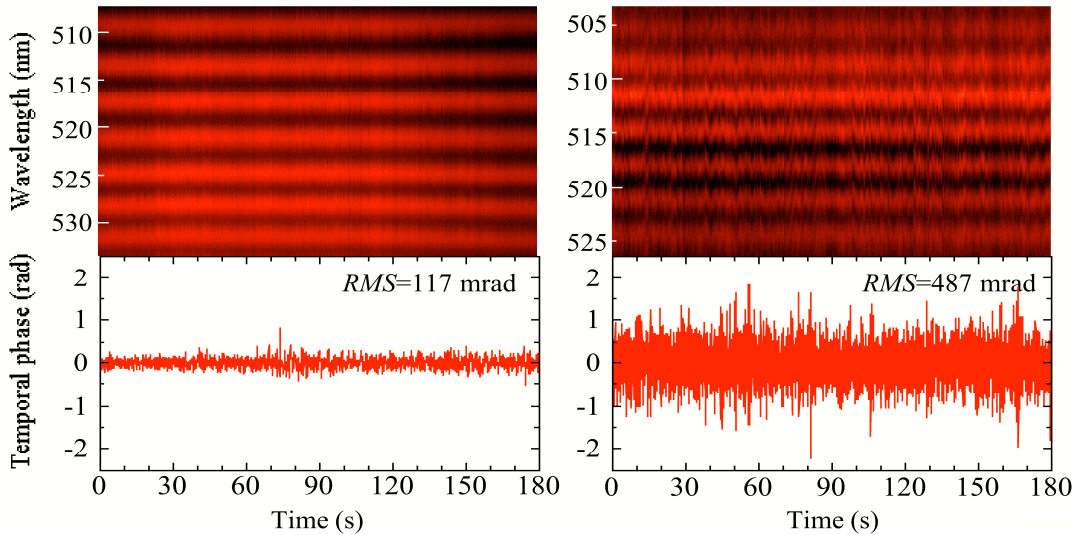


Fig 4.2.4.2

Comparison of the CEP stability of the KLS amplifier (left) and a Neon filled hollow-core fiber pumped by the KLS amplifier. The KLS amplifier had an RMS CEP stability of 117mrad, while the Neon fiber had an RMS CEP stability of 487mrad.

As mentioned previously, it is important for identifying and quantifying the sources of CEP error to simultaneously measure the CEP fringes using both inloop and outloop interferometers.

Preliminary data to this end has been obtained with the Neon fiber. The CEP phase was locked via the oscillator as previously described, and the CEP drift through the amplifier was corrected using the stretcher control method. Inloop and outloop measurements of the CEP stability were made. The inloop measurement was made using 10% of the output of the KLS amplifier, while the outloop measurement was made using the output of the Neon fiber. The KLS power was stabilized to a standard deviation of 0.6%. This compared to an unstabilized standard deviation of about 1.2%. The inloop

measurement showed a rms deviation of the CEP to be 190mrad and the outloop rms deviation to be 370mrad when the power was stabilized. When the power was unlocked outloop rms deviation increased to 550mrad similar to the previous data, suggesting power stability is an important parameter for successful CEP locking. This data represents stability of this level for approximately one minute. This data is shown in Fig 4.2.4.3.

Currently we hypothesize that the CEP fluctuations in the short pulse beam to be dominated fluctuations due to the SPM process in the fiber, and fluctuations resulting from the effect of pointing instability on the coupling efficiency of the fiber. As an example, we expect that fluctuation in the CEP of a fiber pumped to vacuum should be almost entirely due to fluctuations in the beam pointing, with no nonlinear contribution. Further we don't expect this source of error to scale with pressure or input energy. Thus we expect to have an accessible method for obtaining a quantitative measure of the fluctuation due to pointing fluctuations. The error associated with the nonlinear SPM process, however should scale with gas pressure, and input power, potentially in a complicated way. Preliminary efforts to quantitatively express the error in terms of these two errors, which scale in ways that are consistent with what we know about the physics of the fiber have not yielded qualitatively satisfactory results at this point. A further systematic check of the uncertainty associated with the power meters in the power stability system are also needed to further confirm that the current level of power stability does in fact reduce fluctuations in the CEP due to power instability below the levels associated with the SPM process, and pointing stability.

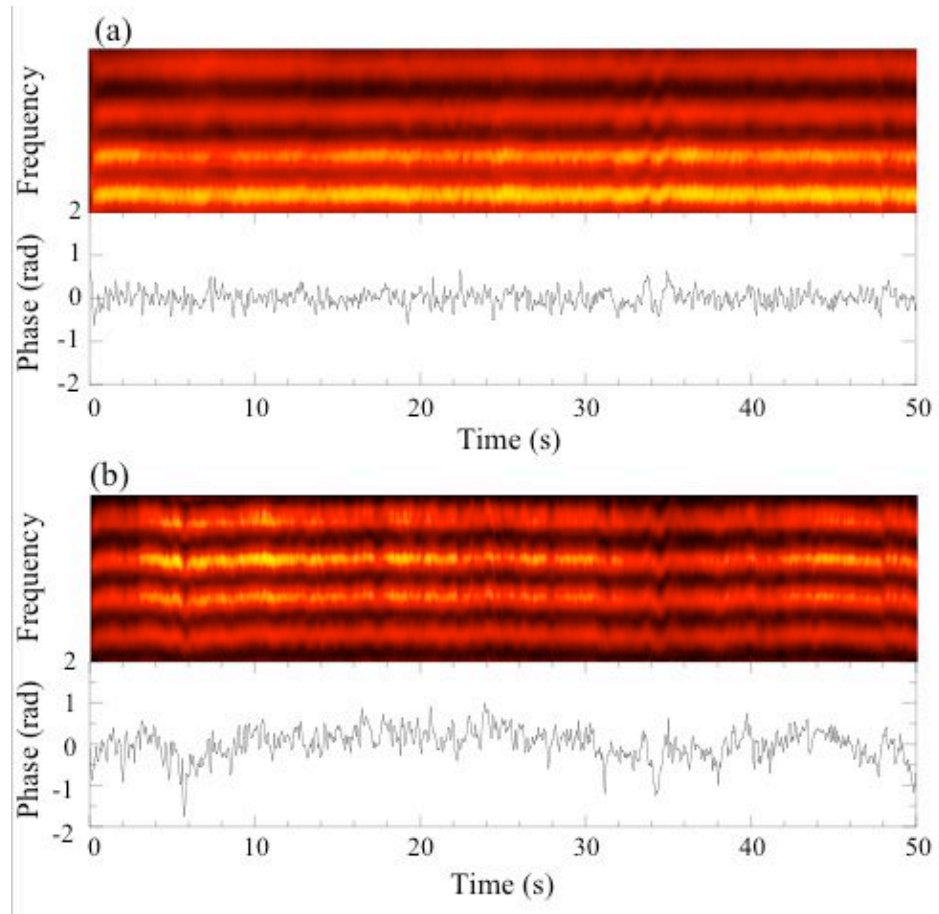


Fig 4.2.4.3

(a) An inloop measurement of the CEP stability of the KLS amplifier shows rms stability at the level of 190mrad. (b) An outloop measurement of the Neon fiber output suggests an rms stability at the level of 370mrad. Power stability had a standard deviation of 0.6% in both cases.

Chapter 5: FROG as a Diagnostic Tool for Ultrafast Lasers

The measurement of the pulse duration of ultrafast laser pulses is a rich field unto itself due mostly to the great importance that pulse duration plays in modern laser-based experiments. At the very least pulse duration must be a known quantity along with pulse energy in order to calculate peak intensity. Although one cannot hope to give a complete treatment of all the techniques available it is necessary to provide a brief discussion of the pulse measurement techniques available in the KLS lab and exploited for this work. We will first discuss the autocorrelator, one of the oldest methods of pulse measurement and then discuss the FROG technique, a newer and quite natural evolution of the autocorrelator.

5.1 The Autocorrelator

Measuring the duration of a short laser pulse has often been complicated by the lack of a shorter event with which to measure the pulse. Autocorrelation, developed in the late 1960's resolved this issue by using the pulse itself as the diagnostic probe[19,20]. In an autocorrelator, Fig. 5.1.1, a pulsed laser beam is split into two equal portions. One of these beams is directed through a variable delay, such as a translatable retro-reflector.

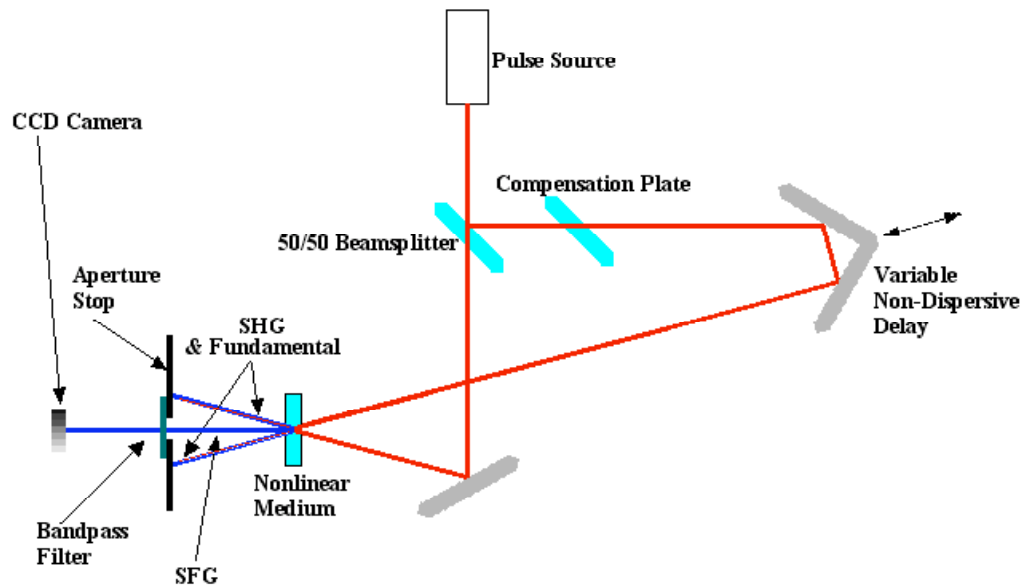


Fig 5.1.1

The basic autocorrelator is the first device for laser pulse duration measurement. In this set-up the pulsed laser beam is split into two components and spatially and temporally overlapped at some angle in a nonlinear medium. The two beams produce SHG along their respective paths and SFG in between. Measuring the SFG intensity as the delay stage is scanned provides a measurement of the autocorrelation width of the pulse.

The two beams are then overlapped in a nonlinear medium. There will typically then be two output beams, which consist of overlapped fundamental output and second harmonic generation (SHG) output. Between these two beams will be a third beam generated by the sum frequency generation (SFG) process. If the beam profiles are small, as would be the case if the beams had to be focused into the nonlinear medium, or if the angle between the entering beams is small, the autocorrelator must make measurements over multiple laser pulses. The delay (τ) is varied while the intensity of SFG is monitored to obtain the autocorrelation trace of the pulse, given by:

$$I_{ac}(\tau) = \int I(t)I(t + \tau)dt \quad (5.1)$$

If the beam profile is sufficiently large and the angle between the two beams is sufficiently large the geometry of the beam overlap itself will generate a delay, which

will vary over the width of the interaction volume. In this configuration the spatial profile of the SFG will yield the time-duration information pulse by pulse. This will be discussed in detail in the next section on FROG. It should be noted that in eq(4.1) the scientist typically does not know the functional form of $I(t)$, and therefore must make some assumption about its functional form in order to actually calculate a value for the duration of either the intensity profile or the envelope of the electric field. In cases where physical constraints cannot be used to determine, with a reasonable degree of certainty, a functional form which $I(t)$ is likely to conform to, this presents a major limitation to the autocorrelation technique. In the next section we discuss the natural solution to this problem: FROG

5.2 Frequency Resolved Optical Gating (FROG)

5.2.1 General Principles of FROG

Although an autocorrelator will give a measurement of a laser pulse's duration there are several significant drawbacks to this technique. The first, as mentioned previously is that one must assume a mathematical form for the pulse in order to extract a pulse duration. This may be reasonable if the pulse is, in reality, well approximated by a Gaussian or $sech^2$ function. If the pulse profile becomes complicated, however such approximations become arbitrary. The second drawback is that the autocorrelator cannot give total information about the pulse's phase. In the best case scenario, that is one has a reasonable confidence in a functional form for $I(t)$, one can obtain many possible electric field assuming phases of various forms of the phase. This is a significant limitation, in the sense that. This information can, however be obtained via another technique, Frequency Resolved Optical Gating (FROG)[21]. In this technique the pulse is

measured, in the so-called time-frequency domain. In this domain we look to measure the spectrogram of the laser pulse. This is given as a two-dimensional function of the pulse frequency and an introduced delay (just as in an autocorrelator):

$$I_S(\omega, \tau) = \left| \int_{-\infty}^{\infty} E(t)E(t - \tau)e^{-i\omega t} dt \right|^2 \quad (5.2)$$

Obtaining a complete description of the electric field from eq (5.2) is known as the 1-D phase retrieval problem, which is not possible without knowledge of $E(t-\tau)$ [21]. It is however possible to cast this in the form of the so-called 2-D phase retrieval problem which is solvable[21]. Thus it is possible to, using FROG completely reconstruct the laser pulse, without making assumptions about the pulse form.

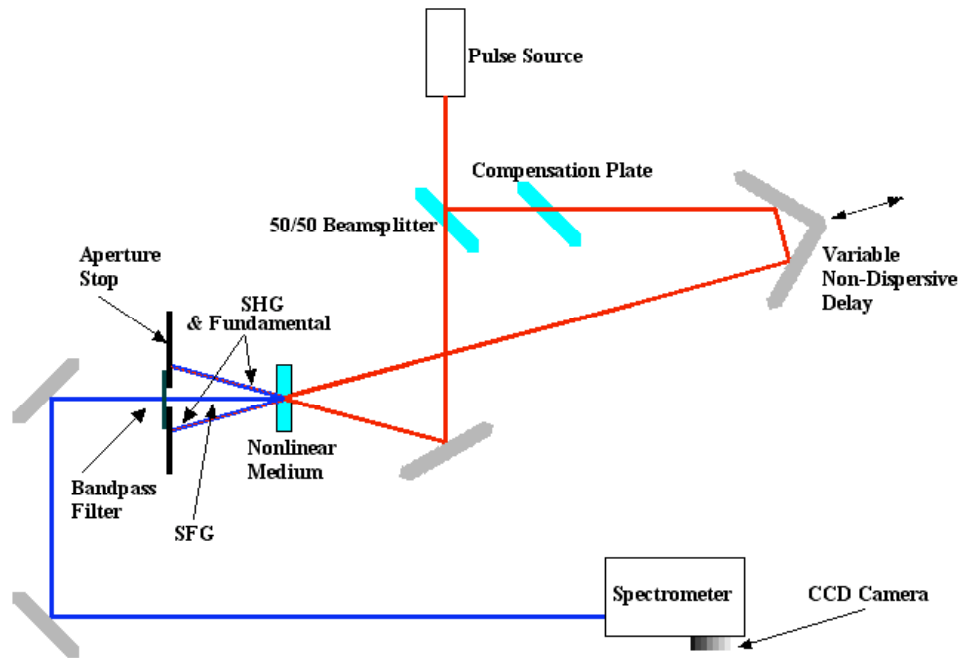


Fig 5.2.1.1

Frequency Resolved Optical Gating (FROG) combines the autocorrelator with a spectrometer allowing for measurement of the 2-D spectrogram. Use of a Fourier transform based phase recovery algorithm allows full pulse reconstruction. Failure of the algorithm to converge provides a good indication of systematic error in the FROG set-up.

The KLS FROG has two important features, which warrant mention. The first is the thin BBO crystal used as the nonlinear medium. This 10 micron thick crystal is necessary to support the bandwidth of pulses shorter than 10fs. To the best of our knowledge there is no commercially available FROG system designed for measurements in that range. The reason for this simply that thinner crystals are capable of phasematching over a broader bandwidth and as such a thin crystal is a pre-requisite for measuring few cycle pulses.

The single shot nature of the KLS FROG also warrants some discussion. For lasers of sufficient intensity that SFG can be generated in sufficient quantities to be detected by the CCD camera without focusing the beams a FROG system can operate as a single shot measurement. If two beams of large diameter are overlapped in a crystal at some angle without being focused, it can be seen from Fig 5.2.2 that a purely geometric delay can be introduced which varies across the wavefronts of the laser beams. Thus making it unnecessary to scan the delay stage. Because of the high power of the KLS beams the KLS FROG can operate in this manner even when measuring the output of a hollow-core fiber compressor.

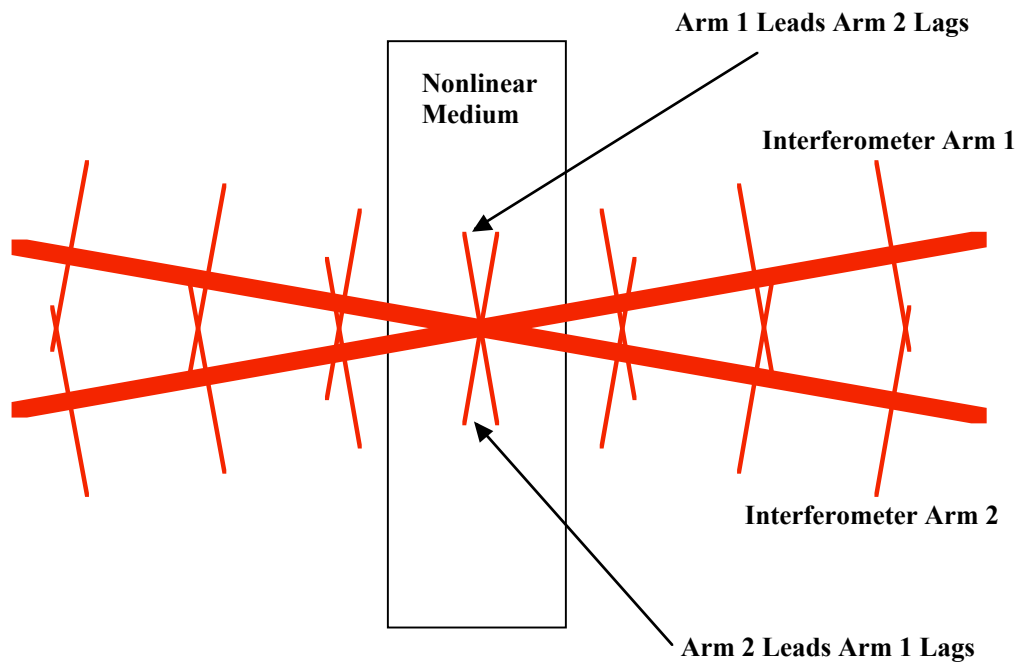


Fig 5.2.1.2

The single shot geometry used in KLS pulse measurement. For lasers of sufficient intensity that the nonlinear process required can occur without focusing the beam a geometric delay can be introduced by way of the finite size of the wavefront. In this figure the thick line symbolizes the propagation direction of the two portions of the laser beam. The thin lines symbolize a line tangent to the wavefront at the center of the beam. The geometric delay is then obvious from the image. In this configuration it is not necessary to vary a delay stage to make the pulse measurement all necessary delay values are measured simultaneously.

5.2.2 Practical Alignment and Calibration of FROG

In this section a general procedure will be outlined for the alignment and calibration of an SHG FROG system. Such a procedure can, for the most part, be broken down into three considerations. The first is the spatial and temporal overlap within the nonlinear medium. The second is calibration of the spectrometer and the third is determining the temporal resolution of the system.

The spatial and temporal overlap can easily be checked by two procedures. Once the two beams seem to be properly aligned and a symmetric spectrogram can be viewed on the CCD camera after the spectrometer proper spatial alignment is achieved if blocking either of the arms of the interferometer completely eliminates the spectrogram. Proper temporal alignment of the FROG is achieved if scanning the delay stage produces: (1) a moving spectrogram in the delay axis (2) a maximum in intensity, which leads to complete extinction at both extremes in delay.

The calibration of the spectrometer is actually a simple procedure. A simple vapor lamp can be used for calibration purposes. In this case an Hg vapor lamp is used because of the large number of lines emitted near 400nm. There are several lines in Hg can be easily observed. In Fig 5.2.2.1 four such lines are shown as captured with the CCD camera in the KLS FROG set-up. On this occasion the FROG was calibrated using the 365.016nm line, though any line could have been used. The calibration was checked for reasonable linearity using the 435.833nm line. The KLS FROG system has a spectral resolution of 0.288nm/pixel using a 121 line/mm grating.

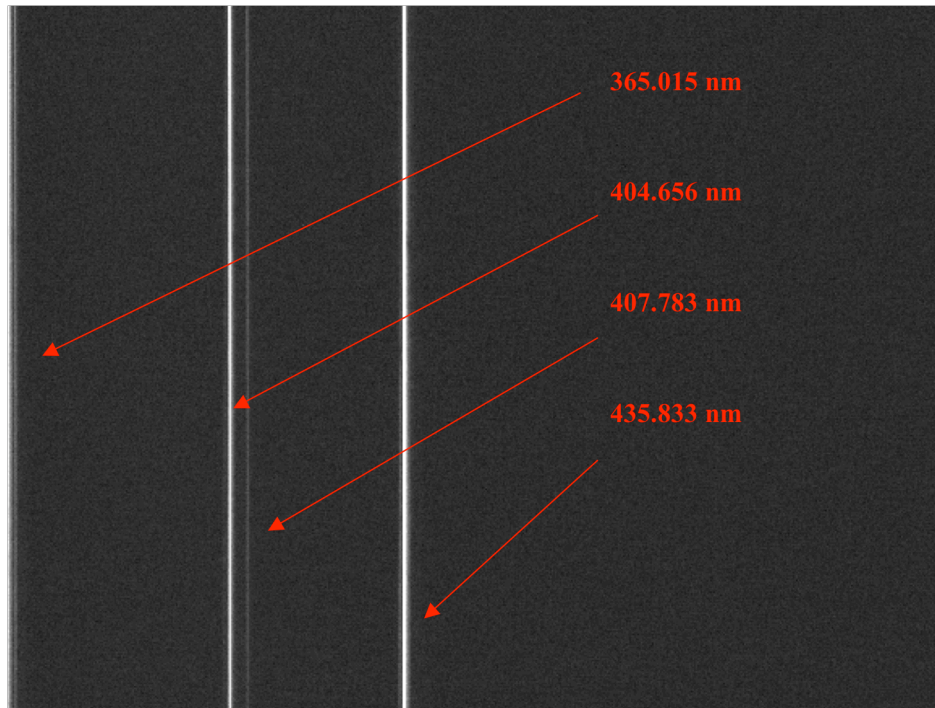


Fig 5.2.2.1

The spectrometer is calibrated using a 365.015nm line from a mercury lamp. The linearity of the calibration is then checked with one of the other lines. The spectrometer has a resolution of 0.288 nm/pixel with this grating.

Determining the temporal resolution of the FROG apparatus is done by slight movement of the delay stage such that the spectrogram moves a small number of pixels along the delay axis, but the intensity doesn't change significantly. Precision measurement of the movement of the delay stage in microns can be achieved. Thus knowing the change in length of one of the arms and the speed of light the total change in delay is calculated. The number of pixels, which the spectrogram moved is then measured and the temporal resolution of the FROG is then the ratio of the number of pixels to the total delay change. Fig 5.2.2.2 shows the movement of the spectrogram induced by an 8 μ m shift of the delay stage. The KLS FROG system has been found to have a temporal resolution of 1.25fs/pixel.

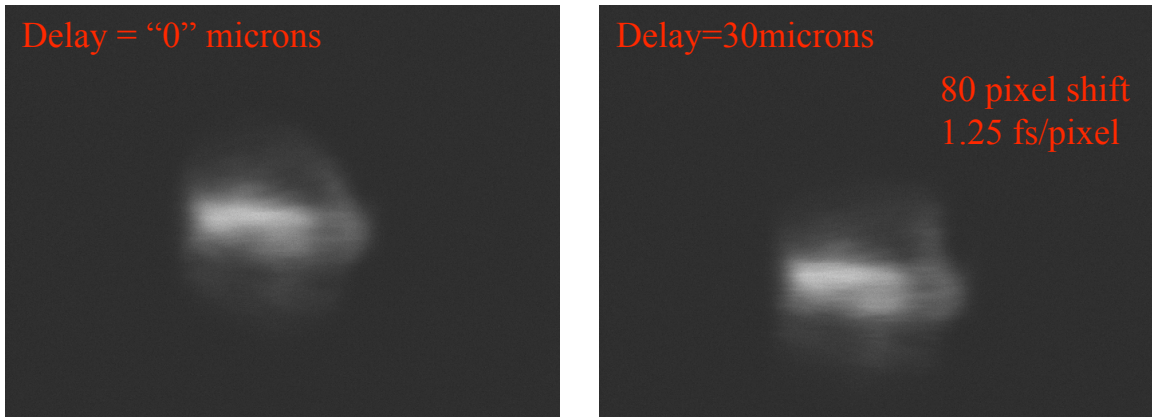


Fig 5.2.2.2

Two sample images showing the adjustment of the delay stage to measure the temporal resolution of the KLS FROG. In this case a movement of approximately 30microns on the delay stage corresponded to 80 pixels of motion, consistent with other measurements of the resolution.

Chapter 6: Application of Neon Fiber Output to HHG CEP Measurements

6.1 Modeling HHG

Focusing intense laser pulses into gases can produce emission of light in high order harmonics of the fundamental laser beam[33,34]. The intensities of these harmonics are constant over many orders, in a region termed the plateau region, and then rapidly decrease in the so-called cut-off region. Harmonics of order 221 have been observed[35]. This process (HHG) can be described by a three-step semi-classical model due to Corkum[36]. In this model the laser first relaxes the coulomb field felt by a bound electron in an atom or molecule. At this point basically two things can happen, dependant on the laser frequency, intensity, and atomic binding energy. If the atomic potential is relaxed sufficiently the electron wavepacket has a significant probability of tunneling through the barrier where it then moves essentially freely under the influence of the laser field. If the barrier is relaxed still further the wavepacket is no longer bound in any significant sense, and the electron moves away from the atomic potential and moves freely under the influence of the laser field. These two types of behavior are shown in Fig 6.1.1.

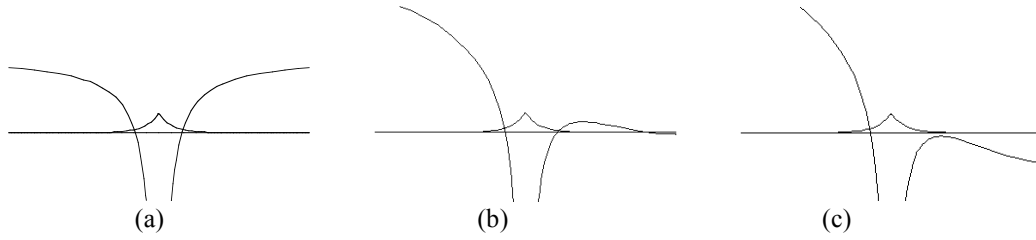


Fig 6.1.1

(a): A depiction of a ground state electron wavefunction in a Hydrogenic atomic potential. (b): The relaxation of the atomic potential in an intense laser field. The potential is relaxed to the point where the electron wavepacket can tunnel through the barrier. (c): The potential is relaxed further due to a more intense laser field. The electron wavepacket is now free without having to tunnel through the barrier.

The critical parameter for distinguishing between these two distinct situations is

the Keldysh parameter given by

$$\gamma = \sqrt{\frac{I_p}{2U_p}} = \sqrt{\frac{4m_e\omega^2 I_p}{e^2 E^2}} \quad (6.1)$$

Where I_p is the ionization potential of the atom and U_p is the ponderomotive energy of the electron in the laser field. In the second equivalency we can see that this relates both to the electric field strength E , and the laser frequency ω . The rule of thumb is that when operating with a Keldysh parameter less than 1 tunneling behavior occurs; when operating with a Keldysh parameter greater than 1 over the barrier behavior occurs. From this information we can predict two important multi-photon phenomena: ATI and HHG. In ATI ionized electrons are emitted with kinetic energies starting from I_p and increasing in integer multiples of the average laser photon energy. In HHG the electron tunnels through, or moves over the relaxed coulomb barrier and moves away from the parent ion under the force of the laser field. One half laser-cycle later the field reverses and the electron is driven back into the parent ion, where it recombines. In this final process a very short burst of radiation in extreme ultraviolet (XUV) region of the spectrum is emitted. This radiation is also in integer multiples of the incident photon

energy ranging from I_p up to $I_p + 3.17U_p$. This ionization and recombination process will occur every half-cycle of the carrier frequency until the envelope of the pulse drops too low to ionize. Thus XUV radiation is created every half-cycle. This can be thought of in temporal analogue to multiple slit diffraction of in the wave-number and position domains. Thus the XUV radiation from each cycle will constructively and destructively interfere in the time domain resulting in an interference pattern in the frequency domain. This interference pattern is the HHG spectrum. As with ATI the HHG's dependence on the electric field strength of the exciting laser gives the opportunity for CE-phase measurement. Changes in the CE-phase will introduce changes in the relative field strength between half cycles of the pulse, changing the contribution of each cycle to the interference pattern in the frequency domain, that is the harmonic spectrum. CE-phase changes will manifest themselves as periodic changes in harmonic intensities and shifting in the energy spectrum.

It then can be realized that if XUV radiation is emitted only during one half-cycle of the laser, the multiple slit analogy becomes a single slit analogy. In this situation the harmonics broaden, overlap and become a broad supercontinuum. The simplest method of limiting HHG to half an optical cycle is a polarization gate in which the laser pulses pass first through a quartz plate aligned such that the polarization of the laser is at 45° to the optical axis, thus generating elliptically polarized light[37-39]. The two components of this light are then each projected onto the axis quarter-wave plate producing right and left circularly polarized light. At the center of this complicated pulse is a linear portion of duration ~ 1.3 fs, or roughly half an optical cycle for most Ti:Sapphire pulsed lasers.

If the intense laser is focused into a large ensemble of atoms it is clear that under some phase matching condition the atoms can, statistically speaking, radiate coherently, thus giving an intense, coherent source of XUV pulses. Due to the large bandwidth associated with an XUV supercontinuum, and the short period of the carrier-frequency XUV radiation from HHG is a promising of isolated attosecond pulses, an important diagnostic tool for understanding electron dynamics on atomic timescales[40-43].

6.2 HHG Experimental Apparatus

In this work HHG in Ar gas was studied using an XUV spectrometer developed for that purpose. The device consists of an evacuated chamber divided into two parts by a gate valve. The laser enters into the first chamber and is focused via a parabolic mirror into an effusive Ar gas jet. In this jet harmonics are produced, which co-propagate with the fundamental toward the gate valve. The gate valve has a 0.5 micron thick Aluminum filter mounted in it. This filter blocks the IR fundamental and acts as a bandpass filter for the XUV light. After passing through the filter the XUV light is directed onto a torroidal diffraction grating, which separates the different harmonic orders and directs them onto a Multi-Channel Plate (MCP) detector. Behind the MCP is a phosphor screen, which is then imaged by a CCD camera. This system is capable of imaging the HHG spectra averaged over many pulses, or by gating the voltage on the phosphor screen it is possible to observe the spectra of a single pulse.

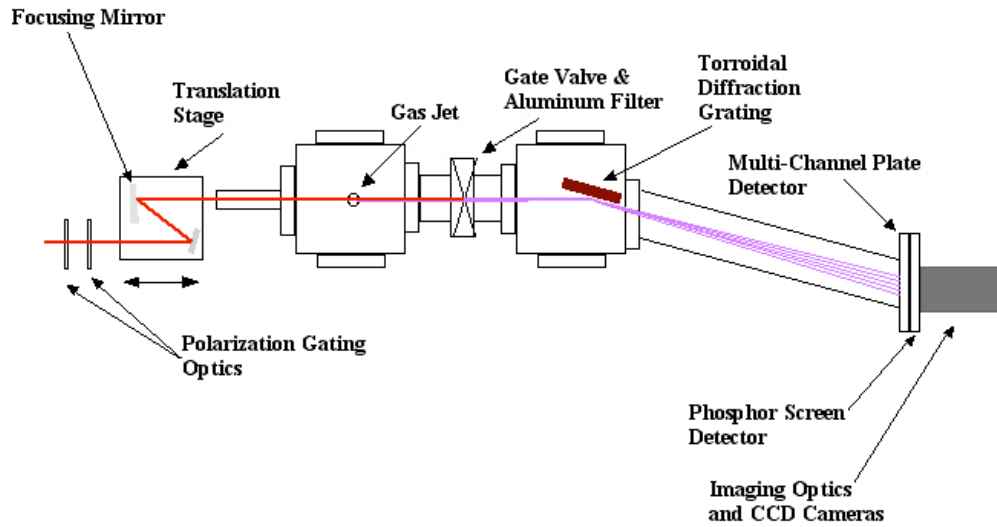


Fig 6.2.1

An XUV spectrometer developed for observing HHG in gases. An ultrafast pulsed laser beam is focused into a gas jet, producing high order harmonics. The laser is then filtered out using an Al filter. The harmonics are separated using a torroidal diffraction grating and projected onto an MCP where they are imaged using a phosphor screen and CCD camera.

In order to observe CEP effects in HHG it is necessary to synchronize the acquiring HHG images with the relative phase measurements made by the f -to- $2f$ interferometer after the amplifier. Since both sets of data are acquired using CCD cameras averaging over many laser pulses, this required that both cameras have the same exposure time, the exposures to be synchronous, and that the data acquisitions begin at the same time. In the acquisition scheme developed for this experiment, a pulse generator (BNC 565 pulse generator) is synchronized with the laser repetition rate (1kHz) via the signal from the first Pockel's cell. This waveform generator then produces a signal $\sim 5V$ and approximately $20\mu s$ duration centered in time on the laser pulse, which acts as a trigger for the Andor CCD camera. The duty cycle of this waveform, however can be controlled, so that for example only every 50^{th} laser pulse is associated with a pulse from the waveform, this coupled with the Andor CCD camera's variable exposure time allows

for triggering exposures which capture many pulses in a precise manner. Both CCD cameras have an output for monitoring the exposure time of the camera, which outputs a signal, which is high while the camera is exposed (exposure time) and low when it is off (down time). Using this monitoring signal from the Andor camera as a trigger for the camera in the f -to- $2f$ interferometer enabled synchronous acquisition. The final step, synchronizing the start and end time of a data file was accomplished programmatically. Both CCD cameras were controlled by LabVIEW routines on two computers. The two computers were connected via serial communication, and the LabVIEW routines were altered such that the signal from the Andor CCD camera would initiate data saving in the f -to- $2f$ interferometer, and that acquisition start-up would initiate data saving in the HHG spectrometer. Monitoring the exposure times via oscilloscope showed synchronization to within $100\mu\text{s}$, much less than the time between laser pulses. This electronic acquisition scheme is depicted in Fig 6.2.2. Fig. 6.2.3(a)-(c) shows oscilloscope traces indicating typical synchronization of the Pockel's cell signal, the gate pulse from the waveform generator, and the exposures of the two CCD cameras.

HHG Electronics Diagram

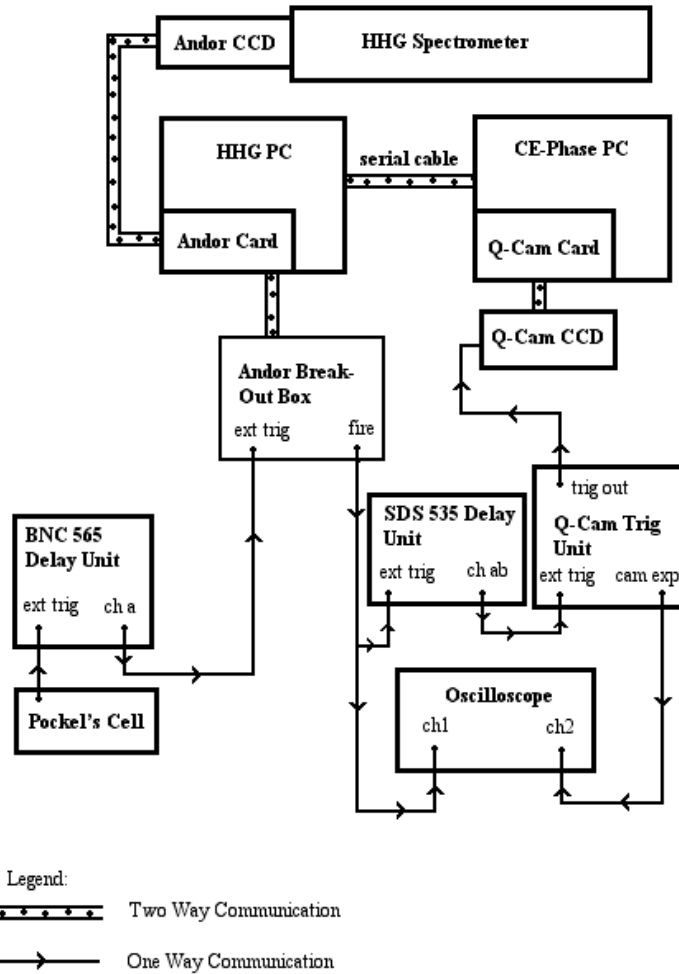


Fig 6.2.2

A graphical depiction of the electronics system for synchronous acquisition of CEP data from the f -to- $2f$ interferometer and the XUV spectrometer is shown. An electronic pulse from the Pockel's cell is the master trigger, a waveform generator turns this signal into a pulse which can trigger the Andor CCD camera, which in turn triggers the CEP CCD camera. LabVIEW and serial communication are used to synchronize acquisition of entire data files. An oscilloscope monitors the synchronization shot to shot.

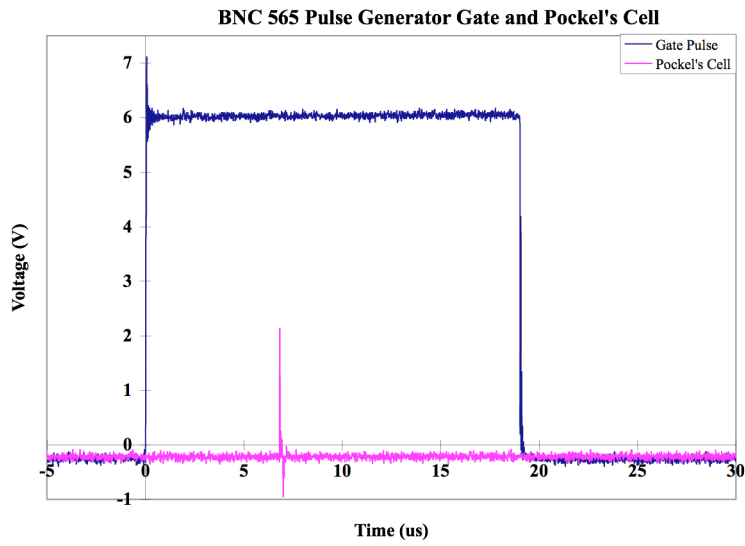


Fig 6.2.3 (a)

The gate pulse from the BNC 565 pulse generator and the Pockel's Cell signal

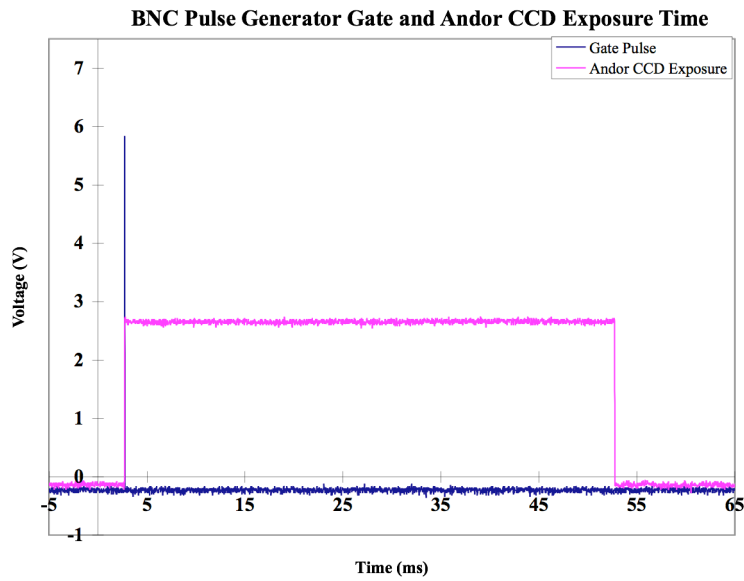


Fig 6.2.3 (b)

The gate pulse from the BNC 565 pulse generator (blue) and the Andor CCD camera exposure set to 50 shots.

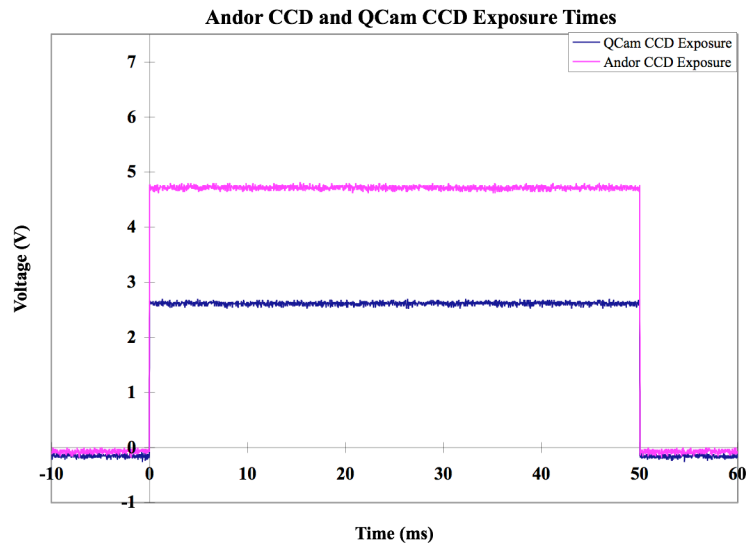


Fig 6.2.3 (c)

The Andor (HHG) and Q-cam (CEP) CCD camera exposure times while both cameras were set to 50ms exposure times as was typical during experiments. Synchronization is better than 200 μ s.

Because the CEP shift effect in the HHG manifests itself in part by changes in the intensity of the harmonic spectrum it is necessary to quantify fluctuations in the laser intensity at the interaction region. These fluctuations can largely be broken down into two effects. The first are simple fluctuations in laser power due to random noise in the amplifier, changes in room conditions, or other causes. The second are changes in the laser pointing which produce an apparent change in intensity at the interaction region. To deal with these two sources of systematic error a monitoring system was devised for both the laser power and the laser pointing.

In this monitoring system a CCD camera was used to monitor the throughput of a chirp mirror. The CCD camera image was then acquired via LabVIEW and a thin slice was saved for each HHG acquisition. Thus any change in laser pointing would manifest

itself either as a shift of the thin strip, or a change in the length of the strip. At the same time a power meter was set-up to measure a portion of the amplifier output from a 10% beam splitter. This power meter reading was saved via a LabVIEW DAQ card. We can assume that any fluctuations in the amplifier output will only be amplified, not masked by the nonlinear processes in the hollow-core fiber, and thus we have a more sensitive probe of relative changes in the laser power as we save HHG spectra.

6.3 Preliminary CEP Data

CE-Phase effects in HHG have been observed using an Ar filled hollow-core fiber. In this work ~ 1.2 mJ laser pulses were coupled to a hollow-core fiber filled with ~ 0.8 bar of Argon gas to generate short pulses with 0.4-0.6 mJ. These pulses were passed through a polarization gate to generate a pulse with time dependant ellipticity, and a very short linear component at the center of the pulse (~ 1.5 fs). Wedge plates were used to vary the CEP as harmonic spectra were measured. A sample of this type of data is shown in Fig 6.3.1. In this figure it is clear that the harmonics are shifting in energy and intensity as the CEP is varied. This data represents the first observation of the effect of CEP on HHG in the KLS laboratory. Attempting to obtain similar results with a Ne filled fiber should result in higher statistical precision due to higher HHG count rates associated with the factor of two increase in pulse energy when changing from an Ar fiber to a Ne fiber.

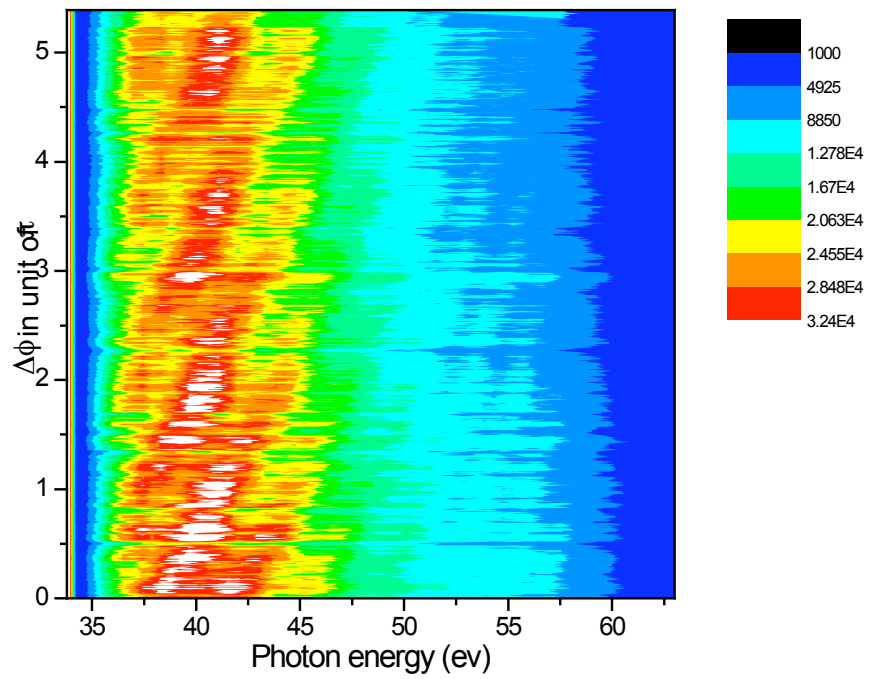


Fig. 6.3.1

CEP effect seen in HHG. Wedge plates are scanned as a gated ultrafast laser pulse is focused into an Argon gas jet. Both a gross periodicity in the intensity of the harmonics is evident as well as finer shifting of the harmonic energy spectrum.

Chapter 7: Conclusions and Future Work

7.1 Conclusions

In this work it is demonstrated that it is possible to generate laser pulses of duration 6.5fs and energy $\sim 1.2\text{mJ}$, using a neon-filled hollow-core fiber. The output of the fiber was shown to have a high beam quality. Techniques for stabilizing the CEP drift of these pulses have also been discussed in the form of synchronized in-loop and out-loop measurements via f -to- $2f$ interferometry. In-loop and out-loop measurements have shown the pulses to have an rms CEP stability of 370mrad as measured in the out-loop. Power stabilization of the KLS has been demonstrated to have a positive effect on CEP stability. Techniques for characterizing such lasers have been discussed as well as the application of such laser pulses to an ultimate goal of measuring the absolute CEP of a laser pulse with HHG. This result is, to the best of our knowledge, the highest energy, most CEP stable pulse generated to date.

7.2 Future Work

There are two main types of work, which continue along the track of this effort. These are efforts to obtain better (shorter, more energetic, etc...) pulses and efforts to use these pulses to perform other scientific experiments. In the realm of generation of better pulses two techniques obviously should be performed in succession to this work. The first is the utilization of the pressure gradient technique to reduce the impact of plasma defocusing and allow for more energetic pulses. The second is the use of the filamentation technique to generate shorter (though lower energy) pulses through self-

compression. All of these pulses can serve as tools for further HHG studies and ultimately attosecond pulse generation, and attosecond time-scale physics experiments.

7.2.1 Pressure Gradient Fibers

Plasma defocusing sets a limit on how much laser pulse energy can be put into a hollow-core fiber compressor while still achieving satisfactory spectral broadening and coupling efficiency[22]. One method of dealing with the plasma defocusing is to reduce the gas pressure that the laser beam is exposed to until it is well coupled to the glass fiber[43]. This can be implemented by drilling a hole into the side of the fiber near its center and using the fiber as a differential pumping aperture. Such a configuration is depicted in fig 7.2.1. In the set-up a seal is formed between the fiber and vacuum chamber at both ends, forming three chambers. Gas is pumped into the fiber through the hole in its side from a high-pressure source and then pumped out via roughing pumps connected to both of the outer chambers. Thus by controlling the rate at which gas is pumped through the system the pressure gradient can be controlled.

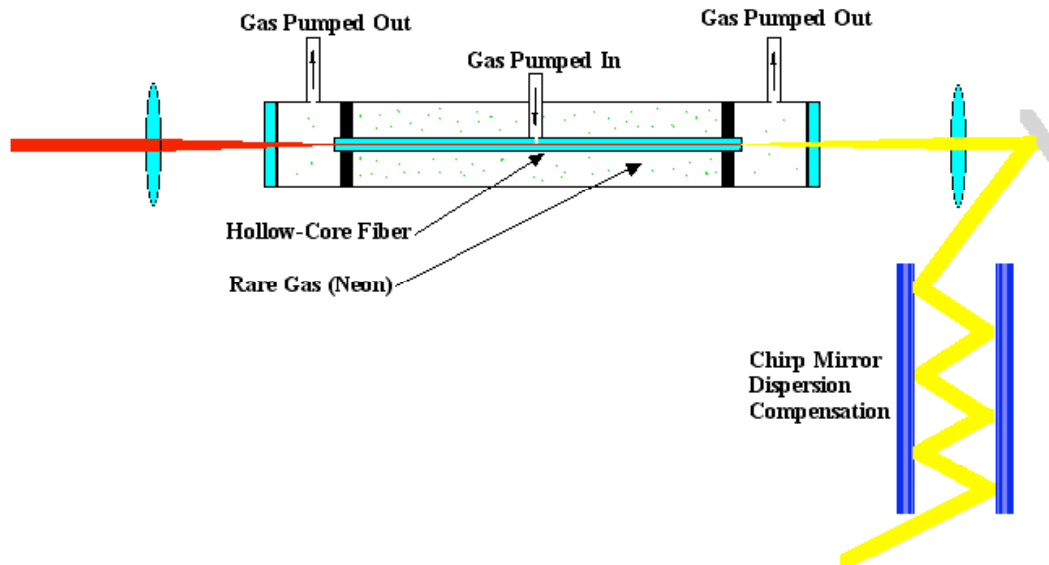


Fig 7.1.1

By using the hollow-core fiber as a differential pumping aperture a pressure gradient across the length of the gas-filled hollow-core fiber can be created. This helps reduce plasma defocusing at the input and exit of the fiber and allows for increased input energy, with higher coupling efficiency. Chirp mirrors again are used for temporal compression of the spectrally broadened pulses.

7.2.2 Pulse Compression via Filamentation

Recently filamentation in noble gases has shown itself to be promising for spectral broadening, and hence short pulse generation[44,45]. Although this method has lower efficiency in terms of laser pulse energy the broader, octave spanning spectrum which can be generated via filamentation is very provides an important simplification for CEP stabilization. Measurement, and correction of the drift of the CEP through a laser system of pulses generated in a CEP locked oscillator makes use of f -to- $2f$ interferometry of an octave-spanning spectrum. Ti:Sapphire laser amplifiers do not normally have octave-spanning spectra, nor do hollow-core fiber compressors. As previously described this has required white light generation in sapphire to generate sufficiently broad spectra and this additional stage can introduce uncertainty as to

whether the f -to- $2f$ measurements actually correspond to the CEP drift of the beam prior to white light generation. If the SPM process used for generating the short pulse also gives the spectrum for the f -to- $2f$ measurement this uncertainty is eliminated. Thus filamentation chambers may be a better source of CEP stable pulses, but with energies perhaps on the 0.3-0.5mJ scale.

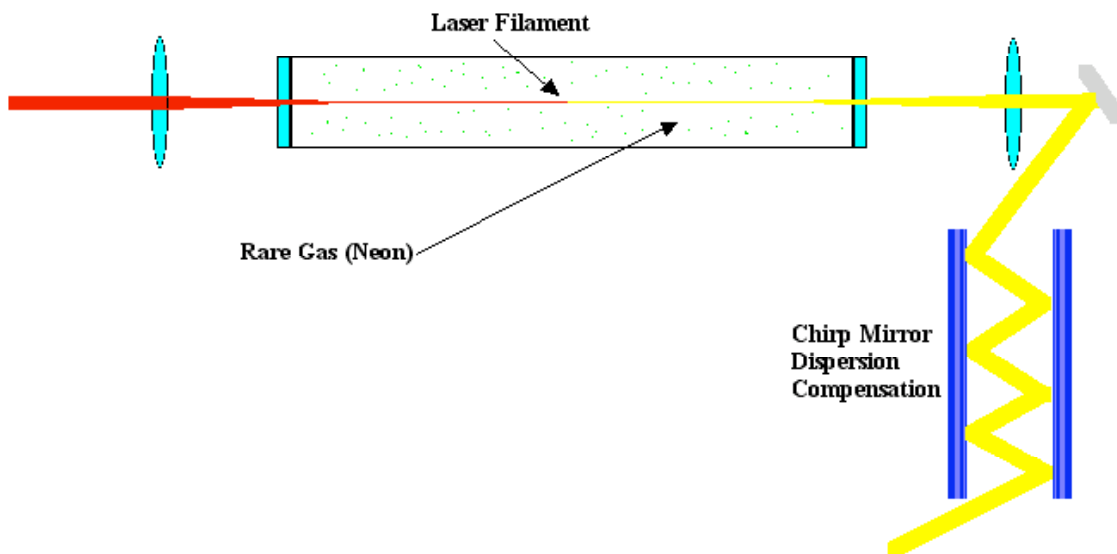


Fig 7.2.1

The Kerr lens generated when an intense laser beam is focused into a medium with an intensity dependant refractive index can be used to create an intense filament in a gas-filled cell. SPM will occur along the length of the filament allowing spectral broadening. Self-compression in the cell enables generation of short pulses with less chirp mirror compression. The filament is, however sensitive to intensity and is stable when the Kerr lens focusing and plasma defocusing exactly cancel each other out, putting strong limitations on the pulse energy which can be obtained from such a configuration.

7.2.3 Further HHG Investigations

This work must naturally lead to HHG measurements of this same type performed with the laser power measured synchronously and stabilized. The nonlinear process of HHG is most likely more sensitive to power fluctuations, and thus makes a stronger argument for that endeavor. Along the line of further HHG studies it is clear

that a new standard of what it means to lock the CEP could be achieved if measurement of the CEP effects in HHG could be observed on a pulse by pulse basis. This is in part one of the motivating goals of this work. By increasing the pulse energy, which can be obtained from a hollow-core fiber compressor one can increase the harmonic intensity. This is a basic necessity for accurately measuring the harmonic yield from a single laser pulse. Thus the natural evolution of the experiment (performed with the same apparatus shown in Fig 6.2.1) is to focus short pulses with energies greater than 1mJ into a larger volume of gas. In this way the field intensity felt by each atom is the same as for low energy pulses, thus preventing the saturation of the HHG effect, while enabling a larger number of atoms to emit, and increasing the intensity of the spectrum. The phosphor screen is then gated by modulating the applied voltage with a square pulse. With available electronics it is possible to apply this gate at 1kHz, and thus it is the rate at which the CCD camera and computer can transfer and save data, which sets a limit on the rate at which single shot spectra can be measured. With the current set-up every tenth shot is reasonable. Upgrading to a faster camera could result in every fifth or second pulse being captured. This would clearly result in the capability to measure the CEP changes very precisely both in the sense that HHG is sensitive to changes in the CEP, and in the sense that CEP fluctuations could be measured on a nearly pulse-to-pulse basis. Such an experiment would clearly have great implications for strong-field experiments and ultrafast laser science.

References

- [1] T. Brabec and F. Krausz, Review of Modern Physics, **72**, 545 (2000)
- [2] D. Strickland and G. Mourou, Opt. Commun. **56**, 219 (1985)
- [3] M. Nisoli, S. De Silvestri, and O. Svelto, Appl. Phys. Lett **68**, 2793 (1996)
- [4] M. Nisoli, S. De Silvestri, O. Svelto, R. Szipöcs, K. Ferencz, Ch. Spielmann, S. Sartania, and F. Krausz, Opt. Lett. **22**, 522 (1997)
- [5] S. Ghimire , B. Shan, C. Wang, and Z. Chang, Laser Phys. **15**, 838 (2005)
- [6] A. J. Verhoef, J. Seres, K. Schmid, Y. Nomura, G. Tempea, L. Veisz, and F. Krausz, Appl. Phys. B **82**, 513 (2006)
- [7] T. M. Fortier, D. J. Jones, J. Ye, and S. T. Cundiff, IEEE J. Select Topics Quantum. Electron. **9**, 1002 (2003)
- [8] S. T. Cundiff, J. Phys. D, **35**, R43 (2002)
- [9] A. Baltuska, M. Uiberacker, E. Gouliemakis, R. Kienberger, V. S. Yakovlev, T. Udem, T. W. Hansch, and F. Krausz, IEEE J. Select Topics Quantum. Electron. **9**, 272 (2003)
- [10] E. Moon, C. Q. Li, Z. Duan, J. Tackett, K.L. Corwin, B. R. Washburn, and Z. Chang Optics Exp. **14**, 9758 (2006)
- [11] Z. Chang, Appl. Opt. **45**, 8350 (2006)
- [12] C. Q. Li, E. Moon, and Z. Chang Opt. Lett. **31**, 3113 (2006)
- [13] C. Q. Li, E. Moon, H. Mashiko, C. M. Nakamura, P. Ranitovic, C. M. Maharjan, C. L. Cocke and Z. Chang, Opt. Express **14**, 11468 (2006)
- [14] R. Trebino, K. W. DeLong, D. N. Fittinghoff, J. N. Sweetser, M. A. Krumbugel, B. A. Richman, and D. J. Kane, Rev. Sci. Instrum. **68**, 9 (1997)
- [15] P. Dietrich, F. Krausz, and P. B. Corkum, Opt. Lett. **25**, 16 (2000)
- [16] D. B. Milosevic, G. G. Paulus, W. Becker, Phys. Rev. Lett. **89**, 153001 (2002)
- [17] Z. Chang, Phys. Rev. A, **70**, 043802 (2004)

- [18] I. J. Sola, E. Mével, L. Elouga, E. Constant, V. Strelkov, L. Polleto, P. Villoresi, E. Benedetti, J.-P. Caumes, S. Stagira, C. Vozzi, G. Sansone, and M. Nisoli, *Nature Phys.* **2**, 319 (2006)
- [19] F. Shimizu, *Phys. Rev. Lett.* **19**, 1097 (1967)
- [20] G. P. Agrawal, *Nonlinear Fiber Optics Academic*, San Diego, 2001
- [21] R. W. Boyd, *Nonlinear Optics*, Academic, San Diego, 2003
- [22] C. Vozzi, M. Nisoli, G. Sansone S. Stagira, and S. De Silvestri, *Appl. Phys. B* **80**, 285 (2005)
- [23] M. J. Weber, *Handbook of Optical Materials*, CRC, Boca Raton (2003)
- [24] M. J. Shaw, C. J. Hooker, and D.C. Wilson *Opt. Commun.* **103**, 153 (1993)
- [25] A. E. Siegman, *Lasers University Science Books*, 1986
- [26] P. F. Moulton, *J. Opt. Soc. Am. B*, **3**, 125 (1986)
- [27] D. H. Sutter, G. Steinmeyer, L. Gallmann, N. Matuschek, F. Morier-Genoud, U. Keller, V. Scheuer, G. Angelow, T. Tschudi *Opt. Lett.* **24**, 631 (1999)
- [28] D. E. Spence, P. N. Kean, W. Sibbett, *Opt. Lett.* **16**, 42 (1991)
- [29] E. A. Marcatili and R. A. Schmelzter *Bell Syst. Tech. J.* **43**, 1783 (1964)
- [30] M. Maier, W. Kaiser, and J. A. Giordmaine, *Phys. Rev. Lett.* **17**, 1275 (1966)
- [31] H. P. Webber, *J. Appl. Phys.* **38**, 2231 (1967)
- [32] C. Iaconis, and I. A. Walmsley, *Opt. Lett.* **23**, 792 (1998)
- [33] A. McPherson, G. Gibson, H. Jara, U. Johann, T. S. Luk, I. A. McIntyre, K. Boyer, C. K. Rhodes, *J. Opt. Soc. Am. B*, **4**, 595 (1987)
- [34] A. L'Huillier, K. Schafer, and K. Kulander, *Phys. Rev. Lett.* **66**, 2200 (1991)
- [35] Z. Chang, A. Rundquist, H. Wang, M.M. Murnane, and H. C. Kapteyn, *Phys. Rev. Lett.* **42**, 2967 (1997) and **82**, 2006 (1999)
- [36] P. B. Corkum, *Phys. Rev. Lett.* **71**, 1994 (1993)
- [37] M. Ivanov, P. B. Corkum, T. Zou, and A. Bandrauk, *Phys. Rev. Lett.* **74**, 2933 (1995)

- [38] P. B. Corkum, N. H. Burnett, and M. Y. Ivanov, *Opt. Lett.*, **19**, 1870 (1994)
- [39] B. Shan, S. Ghimire, and Z. Chang *J. Mod. Opt.* , **52**, 277(2005)
- [40] A. Baltuska, Th. Udem, M. Uiberacker, M. Hentschel, E. Goulielmakis, Ch. Gohle, R. Holzwarth, V.S. Yakovlev, A. Scrinzi, T. W. Hänsch, and F. Krausz, *Nature*, **421**, 611 (2003)
- [41] Z. Chang, *Phys. Rev. A* **71**, 023813, (2005)
- [42] J. H. Carrera, X. M. Tong, and S. I. Chu, *Phys. Rev. A* **74**, 023404 (2005)
- [43] J.H. Sung, J. Y. Park, T. Imran, Y.S. Lee, and C. H. Nam, *Appl. Phys. B* **82**, 5 (2006)
- [44] A. Couairon, J. Biegert, C.P. Hauri, W. Kornelis, F.W. Helbing, U. Keller, and A. Mysyrowicz, *J. Mod. Opt.* **53**, 10 (2006)
- [45] A Guandalini, P. Eckle, M. Anscombe, P. Schlup, J. Biegert, and U. Keller *J. Phys. B*, **39**, 257 (2006)

Associated Publications

- [1] Hiroki Mashiko, Christopher M. Nakamura, Chengquan Li, Eric Moon, He Wang, Jason Tackett, and Zenghu Chang “Carrier-envelope phase stable 5.6 fs pulsed with energy of 1.2 mJ” Applied Physics Letters (submitted)

- [2] Chenquan Li, Eric Moon, Hiroki Mashiko, Christopher M. Nakamura, Predrag Ranitovic, Chakra, M Maharjan, C. Lewis Cocke, Zenghu Chang, and Gerhard G. Paulus “Precision Control of Carrier Envelope Phase in Grating Based Chirped Pulse Amplifiers” Optics Express, Volume 14, p.11,468 (2006)

- [3] He Wang, Chengquan Li, Jason Tackett, Hiroki Mashiko, Christopher M. Nakamura, Eric Moon and Zenghu Chang “Laser Power Locking for Improved Carrier Envelope Phase Stability” Optics Letters (submitted)

- [4] Chengquan Li, Eric Moon, He Wang, Hiroki Mashiko, Christopher M. Nakamura, Jason Tackett, and Zenghu Chang, “Determining the Phase-Energy Coupling Coefficient in Carrier-Envelope Phase Measurements” Optics Letters (submitted)